The Plant Cell, Vol. 29: 3157–3185, December 2017, www.plantcell.org © 2017 ASPB.

The Coiled-Coil and Nucleotide Binding Domains of BROWN PLANTHOPPER RESISTANCE14 Function in Signaling and Resistance against Planthopper in Rice[OPEN]

Liang Hu, Yan Wu, Di Wu, Weiwei Rao, Jianping Guo, Yinhua Ma, Zhizheng Wang, Xinxin Shangguan, Huiying Wang, Chunxue Xu, Jin Huang, Shaojie Shi, Rongzhi Chen, Bo Du, Lili Zhu, and Guangcun He[1]

State Key Laboratory of Hybrid Rice, College of Life Sciences, Wuhan University, Wuhan 430072, China

ORCID ID: 0000-0001-6395-4774 (G.H.)

***BROWN PLANTHOPPER RESISTANCE14* (*BPH14*), the first planthopper resistance gene isolated via map-based cloning in rice (*Oryza sativa*), encodes a coiled-coil, nucleotide binding site, leucine-rich repeat (CC-NB-LRR) protein. Several planthopper and aphid resistance genes encoding proteins with similar structures have recently been identified. Here, we analyzed the functions of the domains of BPH14 to identify molecular mechanisms underpinning BPH14-mediated planthopper resistance. The CC or NB domains alone or in combination (CC-NB [CN]) conferred a similar level of brown planthopper resistance to that of full-length (FL) BPH14. Both domains activated the salicylic acid signaling pathway and defense gene expression. In rice protoplasts and *Nicotiana benthamiana* leaves, these domains increased reactive oxygen species levels without triggering cell death. Additionally, the resistance domains and FL BPH14 protein formed homocomplexes that interacted with transcription factors WRKY46 and WRKY72. In rice protoplasts, the expression of FL BPH14 or its CC, NB, and CN domains increased the accumulation of WRKY46 and WRKY72 as well as WRKY46- and WRKY72-dependent transactivation activity. WRKY46 and WRKY72 bind to the promoters of the receptor-like cytoplasmic kinase gene *RLCK281* and the callose synthase gene LOC_Os01g67364.1, whose transactivation activity is dependent on WRKY46 or WRKY72. These findings shed light on this important insect resistance mechanism.**

INTRODUCTION

Almost 400,000 species of plant-eating insects have been identified (Schultz, 2002), and every known plant species is attacked by a range of insect species. For example, hundreds of insect species are known to feed on rice (*Oryza sativa*), ~30 of which can cause severe damage to rice plants (Grist and Lever, 1969). To survive, plants have evolved sophisticated systems for defense against or resistance to such insects. Recently, significant progress has been made toward understanding the genetic basis of plant resistance to insect attack. Several planthopper resistance genes (including *BROWN PLANTHOPPER RESISTANCE14* [*BPH14*], *BPH26*, *BPH18*, and *BPH9*) have been isolated and shown to encode CC-NB-LRR (CNL) proteins (Du et al., 2009; Tamura et al., 2014; Ji et al., 2016; Zhao et al., 2016). Other notable insect resistance genes have similar CC-NB-LRR structures, including *Mi-1.2* in tomato (*Lycopersicon peruvianum*) and *Vat* in melon (*Cucumis melo*), which confer resistance to aphids (*Macrosiphum euphorbiae* and *Aphis gossypii*), whitefly (*Bemisia tabaci*), and psyllid (*Bactericerca cockerelli*) (Vos et al., 1998; Nombela et al., 2003; Casteel et al., 2006; Dogimont et al., 2014). It thus appears that CC-NB-LRR proteins play prominent roles in plant resistance to insects.

Disease resistance (R) proteins with the CNL structure play central roles in plant-pathogen interactions by recognizing specific pathogen effectors and inducing rapid and robust resistance responses (Jones and Dangl, 2006; Jacob et al., 2013). Consequently, the structures and functions of their domains have been studied extensively. Their C-terminal LRR domains exhibit high sequence variability and appear to function as pathogen-specific receptor domains in at least some cases (Zipfel, 2014). The LRR domains also participate in complex intramolecular interactions that help regulate NLR (nucleotide oligomerization domain [NOD]-like receptor) protein activity (Takken and Goverse, 2012; Slootweg et al., 2013).

The central NB domain of these disease resistance proteins is highly conserved and is found in member of the NB-ARC family of STAND (signal transduction ATPases with numerous domains) proteins (Leipe et al., 2004). The NB domain is believed to act as a molecular switch that stabilizes R proteins in their inactive state when bound to ADP but in the signaling-competent state when bound to ATP (Tameling et al., 2002; Williams et al., 2011). NB domains contain many highly conserved motifs whose functions have been intensively studied. For example, the P-loop is thought to be required for nucleotide binding, and mutations in this motif usually result in loss of function (Tameling et al., 2006; Ueda et al., 2006; Williams et al., 2011). Conversely, the MHD motif acts as a phosphate sensor and is involved in nucleotide-dependent conformational changes; mutations in this motif usually lead to constitutive autoactivation (Bendahmane et al., 2002; Howles et al., 2005; van Ooijen et al., 2008; Gao et al., 2011; Maekawa et al., 2011). Isolated NB domains and CC-NB constructs derived from various CC-NB-LRR proteins have been shown to induce the

[1] Address correspondence to gche@whu.edu.cn.
The author responsible for distribution of materials integral to the findings presented in this article in accordance with the policy described in the Instructions for Authors (www.plantcell.org) is: Guangcun He (gche@whu.edu.cn).
[OPEN]Articles can be viewed without a subscription.
www.plantcell.org/cgi/doi/10.1105/tpc.17.00263

hypersensitive response (HR) in wild tobacco (*Nicotiana benthamiana*) leaves. CC-NB-LRR proteins in this group include Rx (Rairdan et al., 2008) and Sw-5b (De Oliveira et al., 2016) from potato (*Solanum tuberosum*) and RESISTANT TO P. SYRINGAE5 (RPS5) (Ade et al., 2007), RPS2 (Tao et al., 2000), and RPS4 (Zhang et al., 2004) from *Arabidopsis thaliana*. In addition, the NB domains of several disease resistance proteins exhibit nucleotide phosphatase activity consistent with the switch model described above (Fenyk et al., 2012). Interestingly, Rx1 was recently found to bend and locally melt double-stranded DNA in a process mediated by its NB domain (Fenyk et al., 2015, 2016). The functional activity of this NLR protein may thus be linked to a conserved direct interaction with DNA.

CC domains have been implicated in NLR-mediated downstream signaling. These domains might be involved in the recognition of cofactors and cognate effector proteins (Collier and Moffett, 2009; Lewis et al., 2013) or mediate downstream signaling, eventually leading to the induction of defense responses (Maekawa et al., 2011; Collier et al., 2011; Wang et al., 2015a). The HR can be induced via the activation of downstream signaling by isolated CC domains derived from proteins including MLA10 from barley (*Hordeum vulgare*; Maekawa et al., 2011), Rp1-D21 from maize (*Zea mays*; Wang et al., 2015a), Sr33 and Sr50 from wheat (*Triticum aestivum*; Cesari et al., 2016), and NRG1 or ACTIVATED DISEASE RESISTANCE1 (ADR1) from *N. benthamiana* and Arabidopsis (Collier et al., 2011). Since the HR can be induced by the isolated NB domains of Rx1 and Sw-5b, or by the isolated N-terminal CC domain of MLA10, Sr33 and Sr50, it appears that the roles of the CC and NB domains in signaling transduction differ between NLRs.

The recognition of a pathogen effector by a disease resistance protein triggers a strong and multifaceted resistance response often involving the induction of the HR, reactive oxygen species accumulation, defense hormone synthesis, the rapid induction of defense genes, and the production of additional antimicrobial compounds (Jones and Dangl, 2006; Dangl et al., 2013). Recent findings concerning the interactions between disease resistance proteins and associated transcription factors (TFs) have provided important insights into the mechanisms governing the transcriptional activation of nuclear R proteins. In rice, the disease resistance protein Pb1 interacts with the transcription factor WRKY45 through its CC domain to protect WRKY45 against degradation by the 26S proteasome, promoting the accumulation of WRKY45 and, presumably, its defense-related transcriptional activity (Inoue et al., 2013; Matsushita et al., 2013). In Arabidopsis, most WRKY genes are implicated in defense (Dong et al., 2003; Chi et al., 2013).

We previously isolated the brown planthopper resistance gene *BPH14*, which is a CNL gene that confers resistance to brown planthopper (BPH; *Nilaparvata lugens*) and white-backed planthopper (*Sogatella furcifera*) (Du et al., 2009). Here, we present a structure-function analysis of BPH14 protein, which indicates that the isolated CC and NB domains confer BPH resistance and activate salicylic acid (SA) signaling pathways in the same way as the full-length BPH14 protein. We also show that BPH14 and the isolated CC and NB domains interact with WRKY46 and WRKY72, enhancing the accumulation of these transcription factors. We found that WRKY46 and WRKY72 interact with the promoters of *RLCK281* and LOC_Os01g67364.1 and regulate their transactivation. Together, these results provide important insights into the insect resistance mechanism mediated by CNL proteins.

RESULTS

The CC, NB, and CC-NB Domains of BPH14 Confer Resistance to BPH Attack

We previously showed that the brown planthopper resistance gene *BPH14* encodes a CC-NB-LRR protein. To better understand the roles of the BPH14 domains in BPH resistance, we generated a series of BPH14 fragments (Figure 1A). These fragments included the isolated CC, NB, and LRR domains and three constructs featuring two of these domains: CC-NB (CN), NB-LRR (NL), and CC-LRR (CL). The full-length (FL) BPH14 protein was used as a positive control. Constructs expressing these fragments under the control of the ubiquitin (*UBI*) promoter were transformed into the BPH-susceptible *indica* rice variety Kasalath via *Agrobacterium tumefaciens*-mediated transformation. For each transgene construct, we selected two homozygous T2 transgenic lines derived from independent T0 plants that had undergone single-copy insertion (Supplemental Figure 1) for BPH resistance evaluation and further study. In the resistance evaluation, four-leaf stage rice seedlings were exposed to second to third instar BPH nymphs. As soon as the susceptible wild-type rice had been killed by the insects, we evaluated the damage sustained by each plant and assigned a severity score of 0, 1, 3, 5, 7, or 9. We calculated the average scores for each line to quantify their levels of resistance. Transgenic plants expressing the CC domain (CC14-6 and CC22-3), the NB domain (NB9-13 and NB10-9), the CN domain (CN7-18 and CN12-12), or the FL BPH14 protein (FL10-4 and FL12-1) exhibited strong BPH resistance and survived the BPH infestation (Figure 1B). Conversely, lines expressing the LRR domain (LRR2-12 and LRR3-17), the NL domain (NL14-4 and NL18-2), or the CL domain (CL9-6 and CL16-2) showed no resistance to BPH and died after BPH infestation. The average resistance scores for the CC-, NB-, and CN-expressing lines were ~3 to 4, while those for lines expressing the LRR, NL, or CL domains were above 8 (Figure 1C). A BPH14 mutant protein bearing the P-loop K213R mutation (KR7-19, KR15-9 [K is the abbreviation for lysine, while R is the abbreviation for arginine]), which was predicted to render BPH14 inactive, exhibited no BPH resistance (Figures 1B and 1C). Immunoblotting experiments showed that all of the transformed proteins were expressed as expected (Supplemental Figure 2). These results indicate that the CC and NB domains of BPH14 conferred resistance to BPH infestation, as did constructs featuring at least one of these domains. However, the LRR domain conferred no resistance and partially suppressed the resistance conferred by the CC and NB domains.

We performed a series of experiments to determine whether the resistance conferred by the CC and NB domains resulted from antixenosis (which repels insects from its normal host) or antibiosis (which reduces insect survival, growth rate, or reproduction) (Qiu et al., 2011; Smith and Clement, 2012). Host choice tests revealed no significant differences between transgenic and wild-type plants in terms of the numbers of BPH insects that settled on

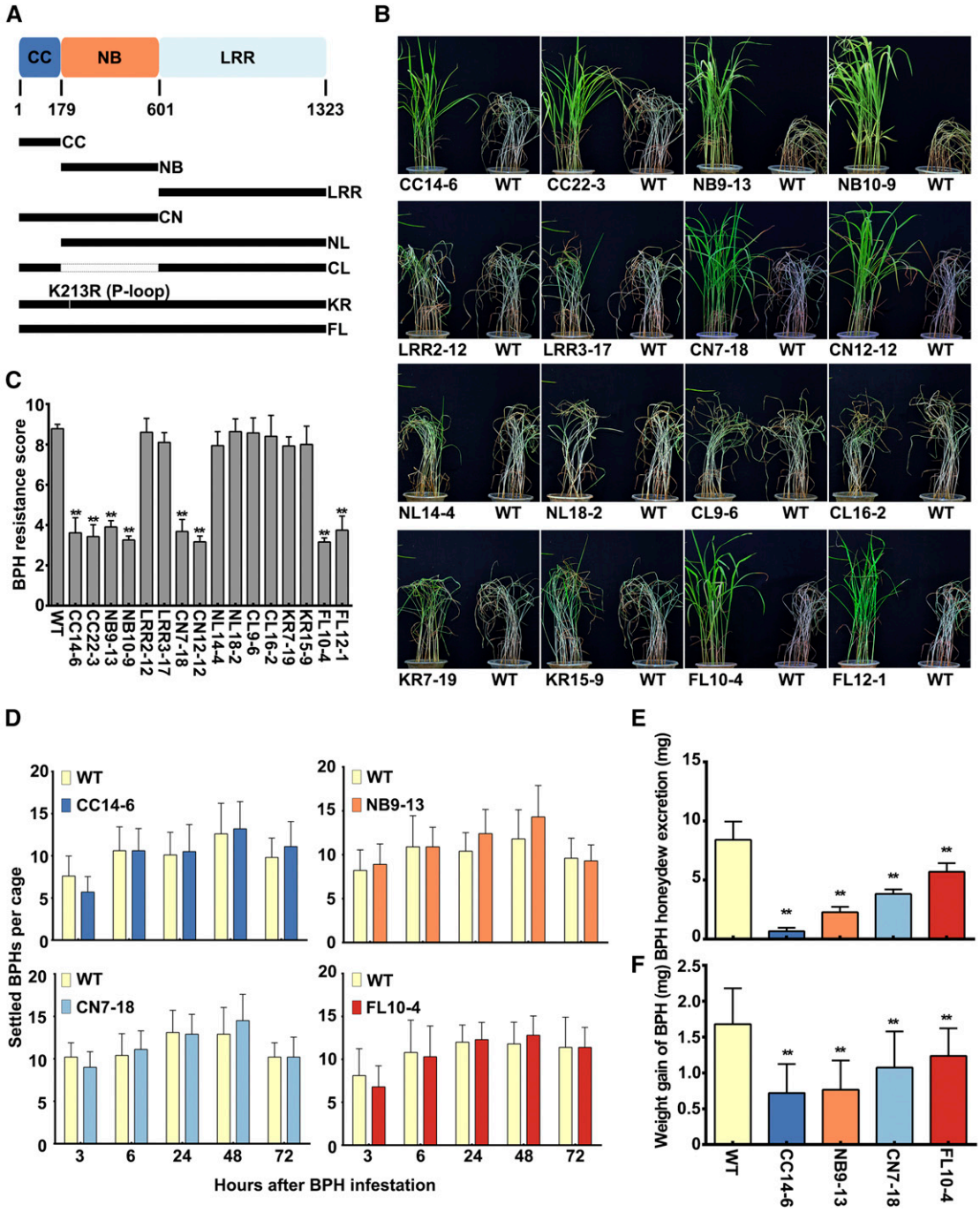

Figure 1. Functional Characterization of the BPH14 CC and NB Domains.

(A) Schematic diagram of the BPH14 domain structure and the derived fragments expressed in the BPH-susceptible Kasalath *indica* variety. Individual domains of BPH14 are represented by colored boxes, and the relative positions of relevant amino acids are indicated. All fragments were transformed into Kasalath rice (under the control of the *UBI* promoter) using the Agrobacterium-mediated method.

(B) BPH resistance phenotypes of transgenic T2 lines expressing BPH14 and its domains. The wild type is Kasalath rice.

(C) BPH resistance scores of transgenic T2 lines expressing BPH14 and its domains. Lower scores correspond to higher levels of insect resistance. Data represent the means (three biologically independent experiments with each experiment having 15 seedlings per rice line used for analysis) ± SD.

(D) Host choice test results for BPH insects on transgenic plants and Kasalath plants. The number of nymphs that settled on the transgenic plants and Kasalath was counted at 3, 6, 24, 48, and 72 h after release. Data represent the means (10 replicates with each repeat having 40 BPH insects per rice line used for analysis) ± SD.

the plants between 3 and 72 h after release (Figure 1D), suggesting that the domains do not act via antixenosis. We investigated antibiosis effects by measuring the quantity of honeydew secreted by the BPH insects. Insects feeding on *CC*, *NB*, *CN*, and *FL BPH14* transgenic plants produced far less honeydew than those on wild-type plants (Figure 1E), and the insects' growth rates and rates of survival were significantly lower when fed on the resistant transgenic plants than on their wild-type counterparts (Figure 1F; Supplemental Figure 3).

We confirmed the functions of the CC, NB, and CN domains in BPH resistance by transforming genes encoding the individual domains, under the control of the native *BPH14* promoter, into Kasalath. The accumulation of the transformed proteins in the transgenic plants was verified by immunoblotting (Supplemental Figure 4A). Subsequent RNA gel blot analysis and qRT-PCR experiments revealed that the resistance domains and FL BPH14 were expressed much more weakly in these native expression lines than in the overexpression lines (Supplemental Figures 4B and 4C). For each resistance domain, we selected two homozygous transgenic plants expressing that domain from the T2 transgenic plants of the native expression lines. The two homozygous T2 transgenic lines for the CC, NB, and CN domains were designated CC6-5 and CC8-4, NB20-2 and NB35-2, and CN1-1 and CN3-18, respectively. We also selected two homozygous plants expressing the FL BPH14 protein (FL9-4 and FL16-2) and used each of these pairs to generate offspring for further analysis. DNA gel blot analyses indicated that all of the resulting offspring exhibited a single-copy insertion (Supplemental Figure 1). Resistance evaluations indicated that the native expression plants retained resistance to BPH (Supplemental Figures 5A and 5B). Moreover, host choice experiments and measurements of BPH honeydew excretion, weight gain, and survival indicated that the resistance mechanism in the native expression lines was the same as that in the overexpressing transgenic lines (Supplemental Figures 6A to 6D). Taken together, these results demonstrate that the CC and NB domains of BPH14 confer resistance to BPH infestation.

We measured the morphological traits of transgenic and wild-type plants. Compared with Kasalath, the overexpressing transgenic lines showed a significant decrease in grain width, grain thickness, and grain weight (Supplemental Figure 7 and Supplemental Data Set 1).

Cell Death Is Not Induced by BPH14, the CC Domain, or the NB Domain

During plant-pathogen interactions, the HR is often triggered by the recognition of a pathogen effector by NLR proteins, which is typical of defense responses in general and usually occurs in tandem with localized programmed cell death (Dangl et al., 2013). Accordingly, the overexpression of some NLR proteins induces cell death in planta (Künstler et al., 2016). To determine whether BPH14 induces cell death in rice, we coexpressed the CC, NB, and CN domains and FL BPH14 with the luciferase reporter protein in rice protoplasts. The luciferase activity in protoplasts transformed with the *CC*, *NB*, and *CN* domains and *FL BPH14* did not differ significantly from those of the empty vector controls (control check [CK]), indicating that BPH14 did not induce cell death in rice (Figure 2A). All of the fusion proteins were properly expressed (Figure 2B).

To verify these results, we transiently expressed the CC, NB, CN, or FL BPH14 constructs in *N. benthamiana* leaves. All of the expected fusion proteins were detected by protein gel blot analysis except for the RPM1 (D505V) protein, which might have been rapidly degraded after the induction of the resistance response (Figure 2C). RPM1 (D505V) rapidly induced HR-like cell death in *N. benthamiana* leaves. However, no detectable cell death was induced by the CC, NB, or CN domains or by FL BPH14 protein, confirming that BPH14 and its CC and NB domains lack cell death-inducing activity (Figure 2D).

The CC and NB Domains of BPH14 Activate the SA Signaling Pathway in Rice

The SA pathway is activated during BPH14-mediated BPH resistance (Du et al., 2009). We found that the transcript levels of the SA biosynthesis-related genes *EDS1* (*ENHANCED DISEASE SUSCEPTIBILITY1*), *PAL1* (*PHENYLALANINE AMMONIA-LYASE1*), *ICS1* (*ISOCHORISMATE SYNTHASE1*), and *NPR1* (homolog of Arabidopsis *NONEXPRESSOR OF PATHOGENESIS-RELATED GENE1*, encoding a key regulator of SA-dependent systemic acquired resistance) were higher in the *CC*, *NB*, and *CN* transgenic plants than in wild-type plants before BPH infestation (except for *PAL1*), and the expression of these four genes further increased after BPH infestation (Figure 3A). *LOX* (*LIPOXYGENASE*) and *AOS2* (*ALLENE OXIDE SYNTHASE2*) encode regulators of jasmonic acid (JA) biosynthesis. The expression of both of these genes was upregulated after BPH infestation in both transgenic and wild-type plants, suggesting that JA-dependent pathways might be involved in the basal defense response to BPH (Figure 3A).

To confirm these findings, we also measured the levels of SA, JA, and JA-Ile in the leaf sheaths of rice plants. The SA concentrations were significantly higher in the *CC*, *NB*, and *CN* domain-expressing transgenic lines than in the wild type and the *FL BPH14* transgenic line before BPH infestation, suggesting that enzymes involved in the biosynthesis of these phytohormones are constitutively expressed in transgenic lines expressing the

Figure 1. (continued).

(E) Honeydew excretion of BPH insects on transgenic plants and Kasalath plants after 2 d. Data represent the means (30 replicates with each repeat having one BPH insect per rice line used for analysis) ± SD.

(F) Weight gain of BPH insects feeding on transgenic plants and Kasalath plants for 2 d. Data represent the means (30 replicates with each repeat having one BPH insect per rice line used for analysis) ± SD.

Data were subjected to ANOVA as detailed in Methods, and asterisks indicate significant differences between transgenic and wild-type plants (*$P \leq 0.05$; **$P \leq 0.01$).

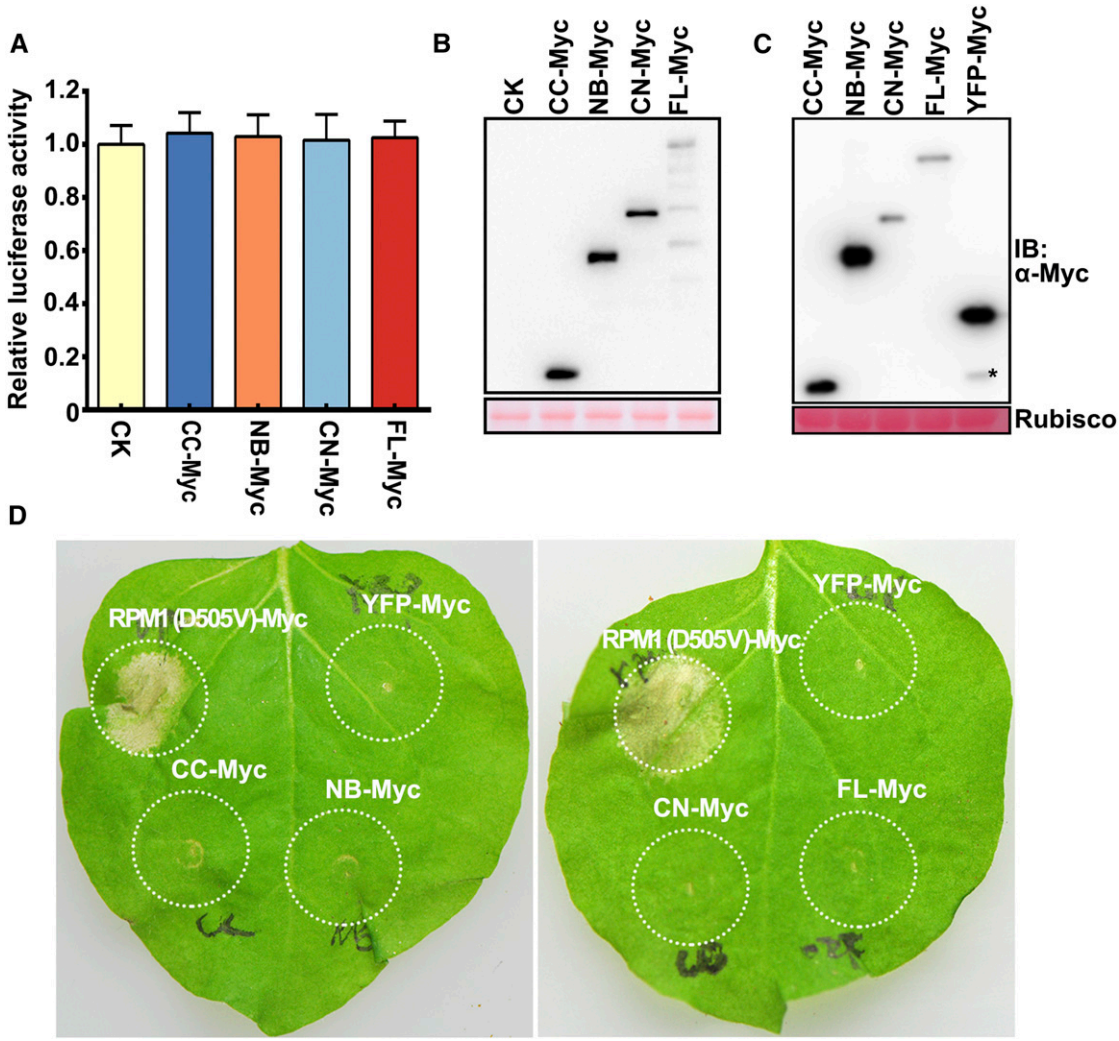

Figure 2. Assessment of Cell Death Induced by BPH14 and Its CC and NB Domains.

(A) Relative LUC activity in rice protoplasts expressing BPH14 and the CC, NB, and CN domains. Protoplasts transformed with empty vector were used as controls (CK). Average values and standard deviations were calculated from eight replicate samples, and values were normalized with respect to the average values of CK. Data were subjected to ANOVA as detailed in the Methods and indicated no statistically significant difference between the protoplasts transformed with the *CC*, *NB*, and *CN* domains and *FL BPH14* and the corresponding control (CK). The experiment was repeated three times, yielding results equivalent to those shown in all cases.

(B) Protein immunoblotting of BPH14 and the CC, NB, and CN domains expressed in rice protoplasts. Ponceau staining of the Rubisco small subunit was used to demonstrate equal loading in all cases except where otherwise specified.

(C) Protein immunoblotting of BPH14 and the CC, NB, and CN domains expressed in *N. benthamiana* leaves. Total protein was extracted from *N. benthamiana* leaves at 48 h after agroinfiltration. Asterisks are used to indicate nonspecific signals throughout this article except where otherwise specified. The autoactivated mutant construct RPM1 (D505V) was not detected because of cell death.

(D) Cell death-inducing activity of BPH14 and the CC, NB, and CN domains in *N. benthamiana* leaves. Cell death symptoms were visualized at 48 h after agroinfiltration. An autoactivated mutant construct, RPM1 (D505V), and a YFP construct were used as positive and negative controls, respectively.

resistance domains. After BPH feeding, the SA levels in transgenic lines expressing the *CC*, *NB*, or *CN* domains, or *FL BPH14*, were significantly higher than in the wild-type plants during the early stages of infestation and increased further during the first 48 h of infestation, followed by a return to basal levels by 72 h after the start of infestation (Figure 3B). The JA levels in the transgenic lines and wild-type plants significantly increased at 3 and 6 h after the start of BPH feeding but returned to the basal levels by 12 h and remained static thereafter (Figure 3B). JA-Ile, the active form of JA, is a major regulatory hormone that controls JA-responsive gene expression and the production of secondary metabolites after biotic stress. The levels of this phytohormone exhibited similar trends to those of JA in the transgenic lines and wild-type plants following BPH infestation, although they increased more rapidly

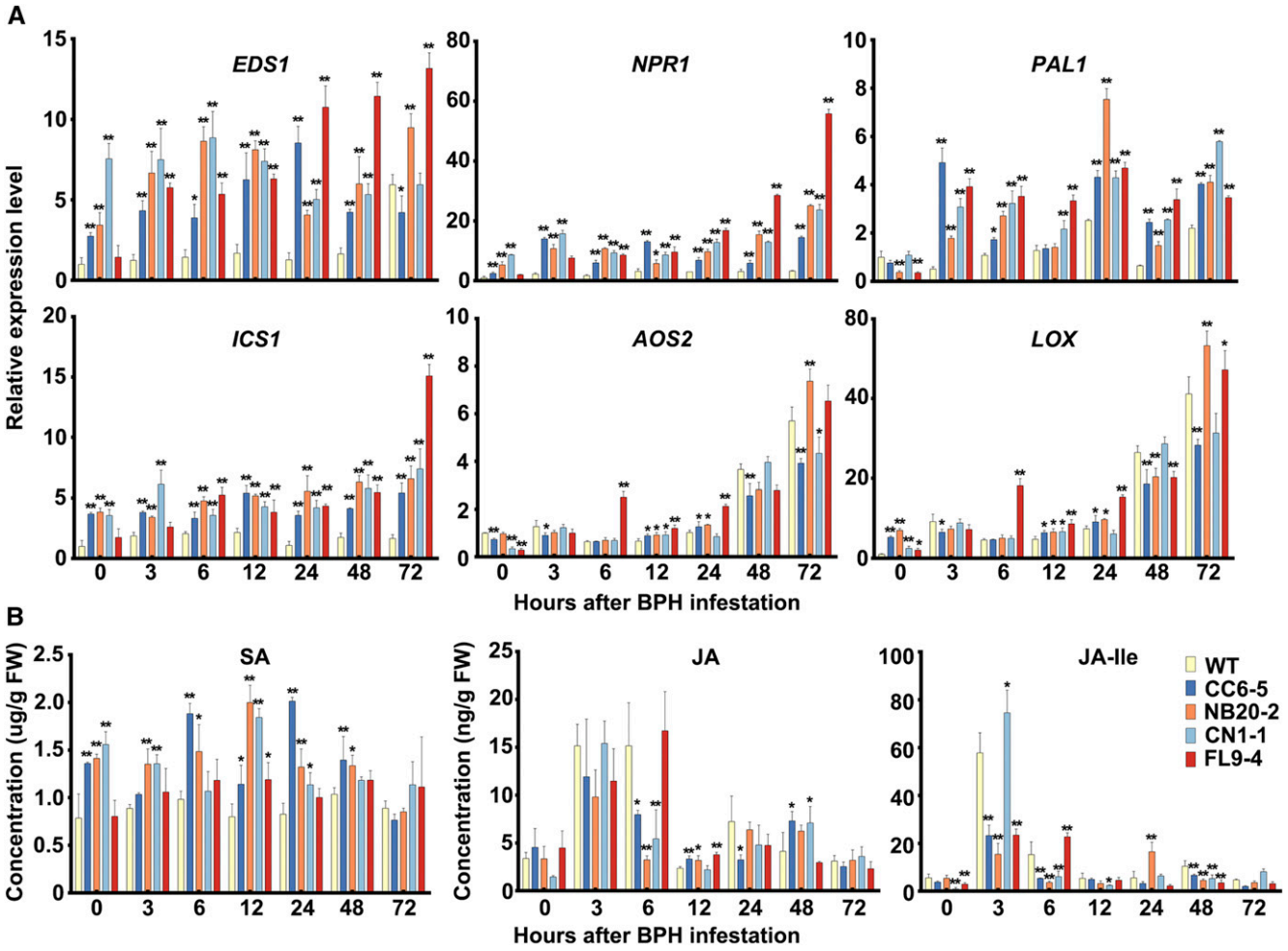

Figure 3. Phytohormone Responses to BPH Feeding in Transgenic Lines Expressing *BPH14* and Its *CC*, *NB*, and *CN* Domains.

(A) Expression analysis of phytohormone-response genes. *EDS1*, *PAL*, and *ICS1* are SA biosynthesis-related genes. *NPR1* encodes a key regulator of SA-dependent systemic acquired resistance. *LOX* and *AOS2* are JA biosynthesis-related genes. Rice *ACTIN1* was used as a reference control. Gene expression was quantified relative to the value obtained from 0-h susceptible samples. Data represent the means (three biologically independent experiments for gene expression) ± SD.

(B) Endogenous levels of SA, JA, and JA-Ile in rice plants. Data represent the means (three biologically independent experiments for hormone concentration) ± SD.

Data were subjected to ANOVA as detailed in Methods, and asterisks show significant differences between transgenic and wild-type plants at the indicated time points after the start of BPH feeding (*P ≤ 0.05; **P ≤ 0.01).

and strongly (Figure 3B). Together with the expression patterns of SA and JA biosynthesis-related genes, these results suggest that the CC and NB domains of BPH14 mildly activate the SA signaling pathway in the absence of BPH feeding and further enhance this activation in response to BPH feeding in rice.

Defense Reactions Are Activated by the CC and NB Domains of BPH14

To characterize the defense responses activated by the CC and NB domains of BPH14, we investigated reactive oxygen species (ROS) generation, defense gene expression, and callose deposition in the transgenic plants after BPH infestation. As before, rice protoplasts were transformed with the *CC*, *NB*, or *CN* domains, or with *FL BPH14*. ROS production was then measured in these protoplasts histochemically using the probe 2′,7′-dichlorodihydrofluorescein diacetate (H_2DCFDA). Rice protoplasts overexpressing the *CC*, *NB*, or *CN* domains, or *FL BPH14*, exhibited significantly more intense green H_2DCFDA fluorescence ($P < 0.01$) than the CK controls, indicating enhanced intracellular ROS accumulation (Figure 4A). A luminol-based extracellular ROS assay revealed that rice protoplasts transfected with an empty vector exhibited no detectable ROS production, whereas those treated with chitin exhibited rapid and transient ROS accumulation within 20 min (Supplemental Figure 8). Protoplasts transfected with constructs harboring the *CC*, *NB*, or *CN* domains, or *FL*

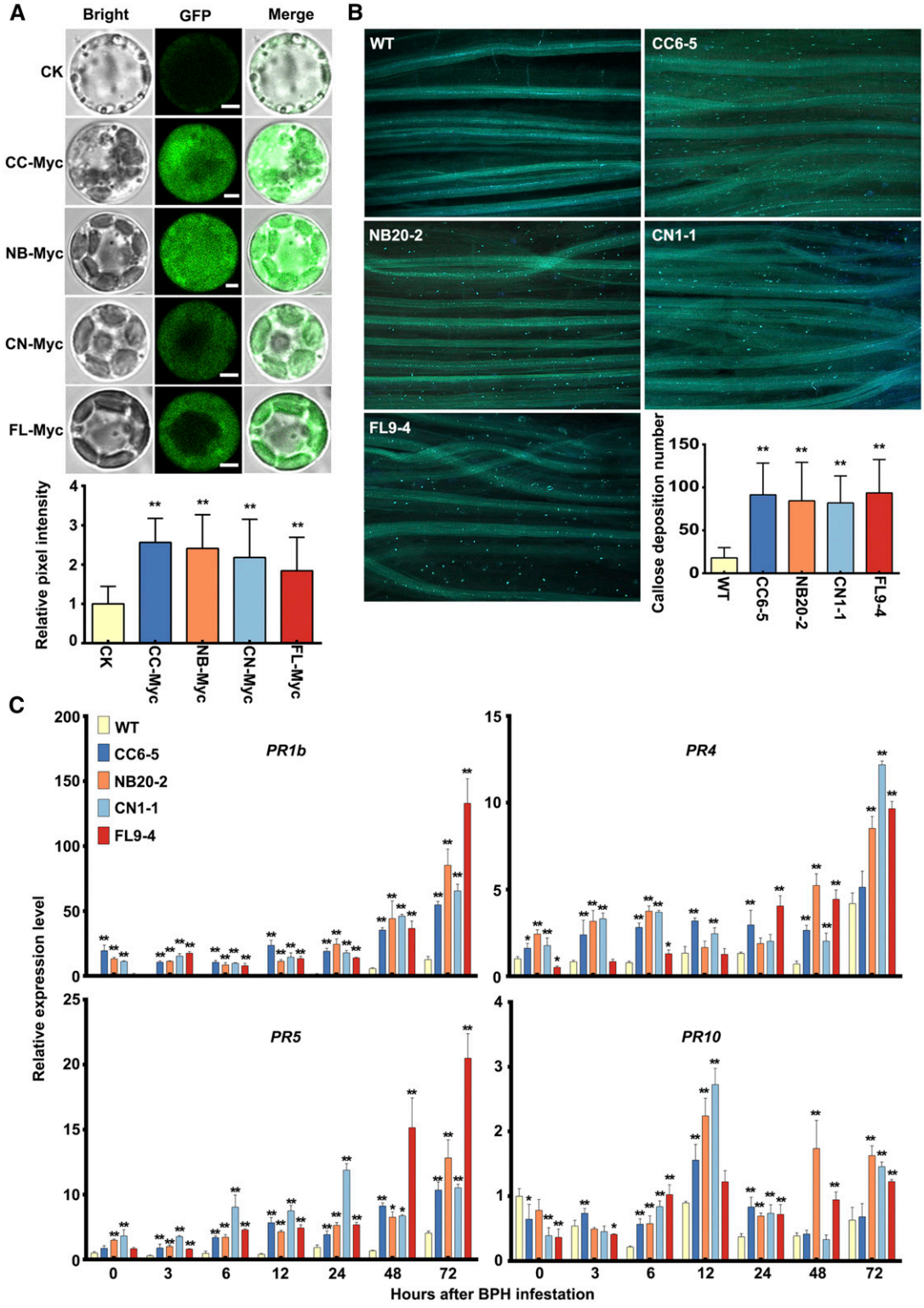

Figure 4. Induction of the Defense Response by the CC and NB Domains of BPH14 in Rice.

(A) Histochemical detection of ROS in intact rice protoplasts. The images (upper) were acquired using an epifluorescence microscope fitted with a GFP filter after rice protoplasts were transfected with the *CC*, *NB*, *CN*, and *FL BPH14* constructs and incubated with the fluorescent probe H_2DCFDA. CK denotes rice protoplasts transfected with the empty vector. Relative pixel intensity (lower) showing corresponding quantification of H_2DCFDA fluorescence in intact

BPH14, exhibited an oxidative burst that was significantly stronger than that of wild-type or CK protoplasts but weaker than that of chitin-treated protoplasts (Supplemental Figure 8). These results indicate that an oxidative burst and enhanced ROS production can be triggered by the isolated CC, NB, or CN domains, and by the FL BPH14 protein.

Callose deposition is an important defense mechanism in *BPH14*-transgenic plants that prevents planthoppers from ingesting their phloem sap (Hao et al., 2008; Du et al., 2009). Transgenic plants expressing the resistance genes exhibited larger and more numerous callose spots than wild-type plants after BPH feeding (Figure 4B). We also examined the expression of callose hydrolase-encoding genes, revealing that *GNS5* and *GNS9* were downregulated in transgenic plants after infestation, but *GNS6* and *GNS8* were not. The effect of these changes is to suppress callose degradation and to ensure that the phloem sieve tubes remain occluded (Supplemental Figure 9). The expression patterns of these genes thus confirmed the reliability of the callose deposition measurements.

The transcript levels of *PATHOGENESIS-RELATED GENE1* (*PR1b*), *PR4*, and *PR5* (but not *PR10*) were constitutively higher in the resistant transgenic lines than in wild-type plants or the *FL BPH14* transgenic line before BPH infestation. Upon BPH feeding, the transcript levels of *PR1b*, *PR4*, and *PR5* increased significantly in the transgenic plants (relative to the wild type) during the first 3 h and remained high after 72 h. Conversely, *PR10* transcript level in the transgenic plants increased significantly at 6 h after infestation, increased further by 12 h, returned to the basal levels between 24 and 48 h, and then increased again by 72 h (Figure 4C). Taken together, these results indicate that the CC and NB domains of BPH14 trigger defense responses including ROS generation, callose deposition, and defense gene activation.

The CC and NB Domains of BPH14 Enhance Plant Resistance to Bacterial Blight

Considering the observation that transgenic plants expressing the *CC* or *NB* domains of BPH14 appeared to exhibit constitutive activation of the SA signaling pathway and defense responses (Figures 3 and 4), we were interested in determining the spectrum of resistance in these plants by including additional pathogens in our assay. We therefore evaluated the resistance level of *CC*, *NB*, *CN*, and *FL BPH14* transgenic and wild-type plants to the bacterial blight pathogen *Xanthomonas oryzae* pv *oryzae* and the fungal blast pathogen *Magnaporthe oryzae*. As expected, compared with wild-type plants, the lesion area caused by *X. oryzae* in *CC*, *NB*, *CN*, and *FL BPH14* overexpressing transgenic plants and transgenic plants with native expression of *CC*, *NB*, and *CN* (but not *FL BPH14*) was significantly reduced (Figures 5A and 5B). However, neither the *CC*, *NB*, *CN*, and *FL BPH14* overexpressing transgenic plants nor the *CC*, *NB*, *CN*, and *FL BPH14* native expressing transgenic plants showed an obvious difference in disease level after *M. oryzae* infection compared with wild-type plants (Figures 5C and 5D). These results suggest that a constitutively induced and primed defense response in transgenic plants may lead to enhanced resistance against the bacterial pathogen *X. oryzae*.

BPH14 Is Localized to the Cytoplasm and Nucleus and Forms Homocomplexes

To determine the subcellular localization of the FL BPH14 protein and its isolated CC, NB, and CN domains, we transiently expressed each protein fused with YFP in rice protoplasts and visualized them by confocal laser scanning microscopy. All four proteins were observed in both the cytoplasm and the nucleus (Figure 6A). Subcellular fractionation of the rice protoplasts revealed that the four proteins were present in both the nuclei-depleted and nuclei-enriched fractions (Figure 6B).

The genes encoding the complete *CC*, *NB*, and *CN* domains and *FL BPH14* were separately cloned into the pGADT7 and pGBKT7 vectors to create a yeast two-hybrid system. The successful expression of each construct in yeast was confirmed by protein gel blot analysis (Supplemental Figure 10A). Experiments using this system revealed that all three individual domains and FL BPH14 formed homocomplexes. Pairwise mating of yeast cells bearing the CC, NB, and CN domains or FL BPH14 with themselves revealed clear positive interactions on a TDO/X-α-Gal/AbA selection plate (Figure 6C). To validate these results in vivo, fusions of the four proteins with a C-terminal HA tag (CC-HA, NB-HA, CN-HA, and FL-HA) were coexpressed in rice protoplasts with fusions of the same protein and a C-terminal Myc tag (CC-Myc, NB-Myc, CN-Myc, and FL-Myc). All of the expected fusion proteins were detected in the transformed rice protoplast extracts by immunoblotting with anti-HA or anti-Myc antibodies, revealing that the input constructs were all properly expressed (Figure 6D) and that the enriched CC-HA, NB-HA, CN-HA, and FL-HA proteins in the output were precipitated by anti-Myc antibodies, suggesting that FL BPH14 and the CC, NB, and CN domains coprecipitated specifically with themselves (Figure 6D). We also prepared pUSYNE-tagged constructs (with split YFP N-terminal fragment

Figure 4. (continued).

protoplasts. The reported values are means (at least 25 protoplasts across ten or more images per genotype from three biologically independent experiments) ± SD. Data were subjected to ANOVA as detailed in Methods, and asterisks indicate significant differences between the protoplasts transformed with the *CC*, *NB*, and *CN* domains and *FL BPH14* and the corresponding control (CK) (*P ≤ 0.05; **P ≤ 0.01). Bars = 5 μm.

(B) Callose deposition in rice plants induced by BPH feeding. The images were taken at 24 h after BPH infestation. Callose deposition values are means (15 replicates) ± SD. Data were subjected to ANOVA as detailed in Methods, and asterisks indicate significant differences between transgenic and wild-type plants (*P ≤ 0.05; **P ≤ 0.01).

(C) Expression patterns of pathogen-related genes in rice plants after BPH infestation. *ACTIN1* was used as a reference control. Gene expression was quantified relative to the value obtained from 0-h susceptible samples. Data represent the means (three biologically independent experiments for gene expression) ± SD. Data were subjected to ANOVA as detailed in Methods, and asterisks show significant differences between transgenic and wild-type plants at the indicated time points after the start of BPH feeding (*P ≤ 0.05; **P ≤ 0.01).

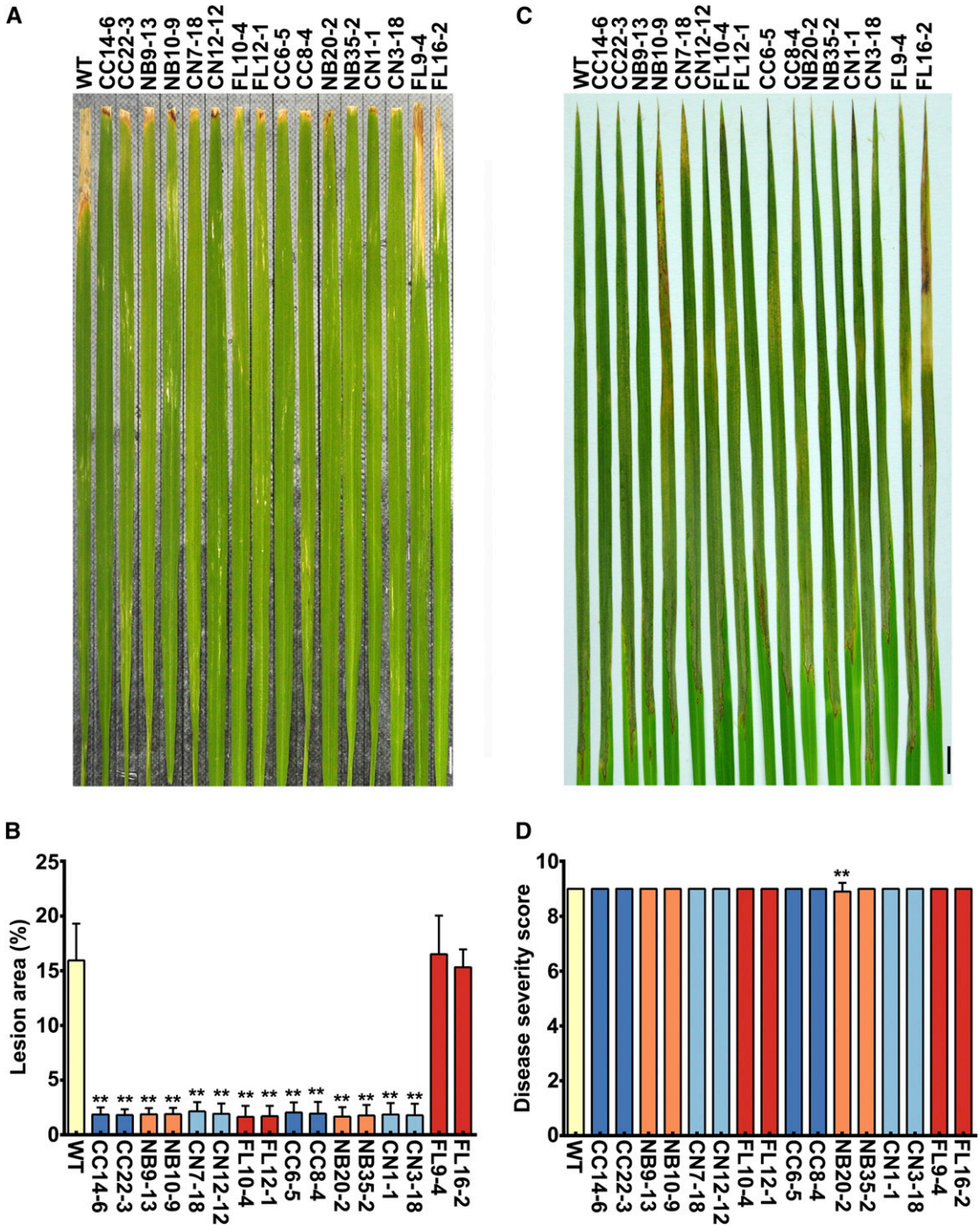

Figure 5. Bacterial and Fungal Pathogen Resistance Test of *CC*, *NB*, *CN* Domain- and *BPH14*-Expressing Transgenic Plants.

(A) Bacterial pathogen resistance phenotypes of wild-type Kasalath and *BPH14*- and *CC*, *NB*, and *CN* domain-expressing transgenic T2 lines infected by *X. oryzae*. Thirty leaves of equal size (the fourth leaf at the four-leaf stage) from each rice line were inoculated with *X. oryzae* (9×10^8 colony-forming units/mL), and phenotypes were recorded in 10 d after inoculation. Bars = 1 cm.

(B) The mean lesion area per leaf (lesion length/leaf length) of the 30 leaves used in **(A)**.

(C) Fungal pathogen resistance phenotypes of wild-type Kasalath and *BPH14*- and *CC*, *NB*, and *CN* domain-transgenic T2 lines infected by *M. oryzae* (1×10^6 colony-forming units/mL). Ten plants at the four-leaf stage from each rice line were inoculated with *M. oryzae*, and phenotypes were recorded in 6 d after inoculation. Bars = 1 cm.

(D) *M. oryzae* disease severity in the investigated rice lines. Higher scores correspond to lower levels of disease resistance.

expression) derived from the FL BPH14 protein and the CC, NB, and CN domains and coexpressed them in rice protoplasts with fusions of the same protein tagged with pUSYCE (giving split YFP C-terminal fragment expression). As expected, the results showed that the CC, NB, and CN domains and the FL BPH14 protein could interact with themselves in both the cytoplasm and nucleus (Figure 6E). These results support the conclusion that the CC, NB, and CN domains, and the FL BPH14 protein, are localized to the cytoplasm and nucleus and form homocomplexes in vivo and in vitro.

BPH14 Interacts with Transcription Factors WRKY46 and WRKY72

To explore the possibility that the role of BPH14 in defense signaling involves direct interactions with rice WRKY TFs such as MLA10 and Pb1 (Shen et al., 2007; Inoue et al., 2013), we performed targeted yeast two-hybrid experiments to investigate the interactions between these proteins. Building on the work of Xie et al. (2005), we gathered information about rice WRKY genes, amplified the cDNA sequences of rice WRKY genes from *indica* rice 9311, and separately cloned these sequences into the pGADT7 vector. *BPH14* was then cloned into the pGBKT7 vector to create a yeast two-hybrid system. We then examined mating combinations involving BPH14 and WRKY46 or WRKY72 and observed a clear positive interaction on the corresponding plates (Supplemental Figure 11). Specifically, combinations in which pGADT7-WRKY46 and pGADT7-WRKY72 mated with pGBKT7-CC, pGBKT7-NB, pGBKT7-CN, or pGBKT7-FL grew well on TDO/X-α-Gal/AbA plates, showing that the CC, NB, and CN domains, and the FL BPH14 protein, all interacted with WRKY46 and WRKY72 in yeast cells (Figure 7A). The identities of the proteins expressed in yeast cells were confirmed by protein gel blot analysis (Supplemental Figures 10B and 10C).

We performed coimmunoprecipitation experiments to confirm the interactions of the CC and NB domains of BPH14 with WRKY46 and WRKY72. To this end, CC-HA, NB-HA, CN-HA, and FL-HA were coexpressed with WRKY46-Myc or WRKY72-Myc in rice protoplasts (Figure 7B). Immunoprecipitation with anti-Myc antibodies caused CC-HA, NB-HA, CN-HA, and FL-HA to coprecipitate with WRKY46-Myc and WRKY72-Myc (Figure 7B), and subsequent immunoblotting assays confirmed that the FL BPH14 protein and its CC, NB, and CN domains all interacted with WRKY46 and WRKY72 in rice cells.

Subcellular fractionation of rice cells from WRKY46- and WRKY72-overexpressing protoplasts revealed the presence of WRKY46 and WRKY72 in nuclei-enriched fractions but not in nuclei-depleted fractions, indicating that both transcription factors were localized to the nucleus (Figures 7C and 7D). To verify the interactions of FL BPH14 and its CC, NB, and CN domains with WRKY46 and WRKY72, we performed bimolecular fluorescence complementation (BiFC) experiments using constructs expressing WRKY46 and WRKY72 tagged with pUSYCE and constructs expressing FL BPH14 or its CC, NB, or CN domains tagged with pUSYNE. In addition, nuclear-localized WRKY74 tagged with pUSYCE was used as a negative control (Supplemental Figure 11) (Dai et al., 2016). The FL BPH14 protein and its domains all interacted with WRKY46 and WRKY72, but not with WRKY74, in the nucleus and YFP signals overlapped with DRN-CFP signals, confirming its nuclear localization (Figure 7E); the proper expression of the fusion proteins of the negative control was verified by protein gel blot analysis (Supplemental Figure 12). In summary, we demonstrated that two transcription factors, WRKY46 and WRKY72, interact with the CC, NB, and CN domains and the FL BPH14 protein in vivo and in vitro. We detected reduced expression of *WRKY46* at 24 and 72 h after the start of BPH feeding in the transgenic lines relative to wild-type plants. However, *WRKY72* transcript levels were significantly higher in the transgenic lines than in wild-type plants between 48 and 72 h after the start of BPH infestation (Supplemental Figure 13).

Binding to BPH14 Stabilizes WRKY46 and WRKY72

When WRKY46 and WRKY72 were expressed in rice protoplasts, the addition of the proteasome inhibitor MG132 resulted in their accumulation, suggesting that both transcription factors are subject degradation by the ubiquitin proteasome system (UPS) in rice cells. Furthermore, coexpression of the CC, NB, or CN domains or the FL BPH14 protein instead of MG132 stabilized WRKY46 and WRKY72 proteins in rice protoplasts (Figures 8A and 8B). Additionally, increasing the levels of FL BPH14 or its CC, NB, or CN domains caused a gradual increase in the accumulation of WRKY46 and WRKY72, but gradually increasing the levels of GFP or truncated GFP derivatives caused no such changes in WRKY protein accumulation (Figures 8C and 8D). These results suggest that the CC, NB, and CN domains and the FL BPH14 protein protect WRKY46 and WRKY72 from UPS-dependent degradation through a protein-protein interaction.

We performed chromatin immunoprecipitation (ChIP) analysis to identify promoters that may interact directly with WRKY46 or WRKY72 in rice protoplasts. After the ChIP test, the enrichment of specific DNA fragments in the immune precipitate was determined by ChIP sequencing. This yielded two sets of ChIP sequencing results, with several common candidate genes as well as several genes that were only enriched by one WRKY protein. Most of these candidate genes are somehow related to defense responses (Supplemental Data Sets 2 and 3). Two that drew our attention were LOC_Os09g39640.1 and LOC_Os01g67364.1. LOC_Os09g39640.1 (*RLCK281*) encodes a receptor-like cytoplasmic kinase (Vij et al., 2008), while LOC_Os01g67364.1 encodes a protein with a glucan synthase component that is predicted to be similar to CALLOSE SYNTHASE5 isoform X1.

Figure 5. (continued).

The data represent the means (30 leaves or 10 plants in each transgenic line used for *X. oryzae* or *M. oryzae* disease resistance analysis for one independent experiments) ± SD. Data were subjected to ANOVA as detailed in Methods, and asterisks indicate significant differences between transgenic and wild-type plants (*P ≤ 0.05; **P ≤ 0.01). Three biological repeats (independent experiments) were conducted.

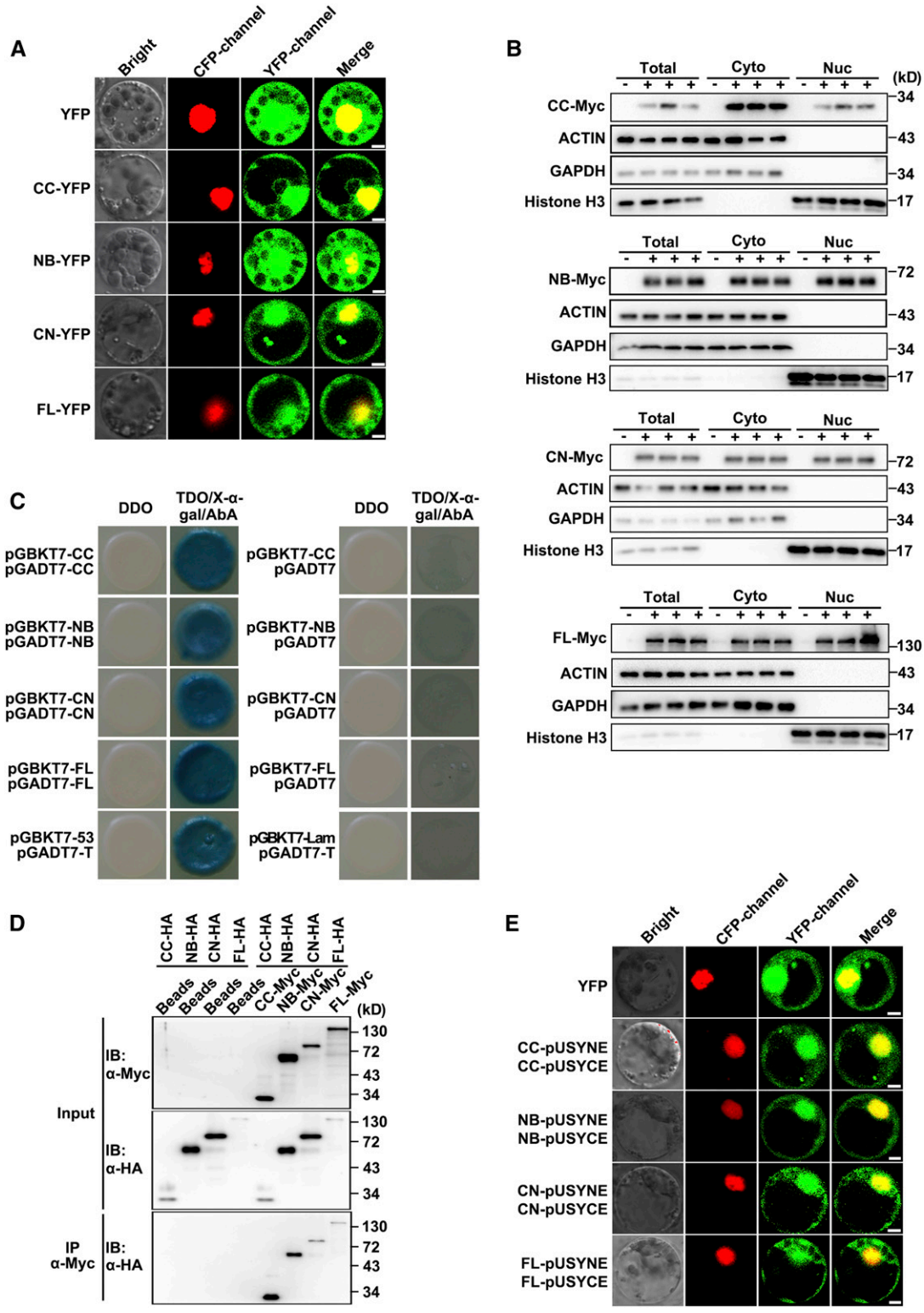

Figure 6. BPH14 Protein Localizes to the Cytoplasm and Nucleus and Forms Complexes.

(A) BPH14 and the CC, NB, and CN domains are localized to the cytoplasm and nucleus of rice protoplasts. DRN-CFP was used as a nucleus marker. Confocal images of protoplasts were taken 16 to 22 h after transfection. Bars = 5 μm.

Bioinformatic analysis of the putative promoter regions (i.e., the sequences 2 kb upstream of the translational start codon) of *RLCK281* and LOC_Os01g67364.1 identified W-box elements (W-box$_{RLCK281}$ and W-box$_{LOC_Os01g67364.1}$) that are recognized by WRKY transcription factors (Supplemental Figure 14). The interactions of WRKY46 and WRKY72 with W-box$_{RLCK281}$ and W-box$_{LOC_Os01g67364.1}$ were verified in by yeast one-hybrid analysis: Yeast cotransformed with WRKYs and W-box$_{RLCK281}$ or W-box$_{LOC_Os01g67364.1}$ grew well in selective medium, indicating that WRKY46 or WRKY72 bound specifically to W-box$_{RLCK281}$ and W-box$_{LOC_Os01g67364.1}$ (Figure 9A). The presence of the DNA bait in the yeast genome and the prey protein in the yeast cells was verified by yeast colony PCR and immunoblotting experiments, respectively (Supplemental Figures 15A and 15B).

Electrophoretic mobility shift assays (EMSAs) revealed that purified 6×His-WRKY46 and 6×His-WRKY72 fusion proteins bound specifically to W-box$_{RLCK281}$ and W-box$_{LOC_Os01g67364.1}$, respectively, but not to the mutant probes (designated mW-box$_{RLCK281}$ and mW-box$_{LOC_Os01g67364.1}$) in which the TGAC sequence of each W-box was changed to TGAA (Figures 9B and 9C; Supplemental Figure 14B) (Yu et al., 2001). The specific probe binding was outcompeted by the respective nonlabeled W-box$_{RLCK281}$ and W-box$_{LOC_Os01g67364.1}$ probes, but not by the mutant probes (Supplemental Figure 16). To assess whether the presence of the CC, NB, and CN domains or FL BPH14 affects the specificity or selectivity of the interacting WRKYs in rice, we expressed WRKY46-Myc or WRKY72-Myc in wild-type and transgenic protoplasts, respectively, and performed ChIP assays using anti-Myc antibody. qPCR analyses of immunoprecipitated chromatin were performed for the promoter region of *RLCK281* and LOC_Os01g67364.1, which harbor W-box$_{RLCK281}$ and W-box$_{LOC_Os01g67364.1}$. Significant enrichment of the DNA segments (CQ1-F/CQ1-R for the *RLCK281* promoter and CQ2-F/CQ2-R for the LOC_Os01g67364.1 promoter) was detected by qPCR in the *CC*, *NB*, and *CN* domains or *FL BPH14*-overexpressing transgenic protoplast samples compared with the wild type (Figures 9D to 9G). Also, coexpression of WRKY46 or WRKY72 with the FL BPH14 protein or its CC, NB, or CN domains enhanced the luciferase activity of the *RLCK281* promoter relative to that detected in the CK control (Figure 9H). Conversely, the luciferase activity of the LOC_Os01g67364.1 promoter was enhanced by coexpression of these domains with WRKY46 but not by coexpression with WRKY72 (Figure 9I). These results strengthen the conclusion that BPH14 plays crucial roles in stabilizing WRKY46 and WRKY72 in rice and that this stabilization enhances the binding of WRKY46 and WRKY72 to the promoter regions of *RLCK281* and LOC_Os01g67364.1 and affects the expression of these candidate defense-related genes.

DISCUSSION

BPH14, a rice gene that confers resistance to the insect brown planthopper, encodes a CC-NB-LRR protein. In this study, we conducted a structure-function analysis of BPH14 protein and demonstrated that plants transformed with genes encoding the *CC* or *NB* domains alone or their combination conferred a similar level of BPH resistance to transgenic lines with the full-length *BPH14* gene. The CC and NB domains of BPH14 activate the SA signaling pathway and defense reactions. Overexpression of the CC, NB, and CN domains and FL BPH14 proteins induced oxidative bursts and enhanced ROS production but without cell death. The CC, NB, CN, and FL BPH14 proteins interacted with themselves and with the transcription factors WRKY46 and WRKY72. ChIP analyses identified the target genes of WRKY46 and WRKY72. We further demonstrated that binding to FL BPH14 or its CC, NB, and CN domains stabilized WRKY46 and WRKY72 and increased WRKY46 and WRKY72-dependent transactivation activity, thus potentiating defense gene expression and immune responses.

The CC and NB Domains Are Necessary and Sufficient for Planthopper Resistance

BPH14 encodes a CNL protein that confers resistance to insect planthoppers. We demonstrated that the CC and NB domains of BPH14 are necessary and sufficient for BPH resistance and signaling pathway activation. In detail, transgenic plants carrying the CC domain, the NB domain, or both exhibited comparable levels of BPH resistance to transgenic plants expressing the complete BPH14 protein. Conversely, transgenic plants expressing the LRR domain or constructs featuring this domain were not resistant to BPH. In general, plants resist insect pests using mechanisms based on antixenosis or antibiosis (Painter, 1951). We previously showed that BPH14 has antibiotic but not antixenotic activity toward BPH insects (Du et al., 2009). Here, we found that transgenic plants expressing the CC and NB domains also exhibited an antibiotic but not an antixenotic effect toward BPH, suggesting that the individual domains induce the same resistance mechanism as BPH14. We therefore conclude that the BPH14 CC and NB domains constitute minimal functional modules for BPH resistance initiation. Other disease resistance protein

Figure 6. (continued).

(B) Protein gel blot analysis of BPH14 and the CC, NB, and CN in cytoplasm (Cyto) and nucleus (Nuc) fractions. Nuclei-depleted and nuclei-enriched fractions were prepared from rice protoplasts and analyzed by protein gel blot analysis. Ten-fold equivalents of nuclei-enriched fractions were used relative to the nuclei-depleted fractions. BPH14 and the CC, NB, and CN domains were detected in nuclei-depleted and nuclei-enriched fractions using anti-Myc antibody. Histone H3 was used as a nucleus marker, and ACTIN and GAPDH as cytoplasm markers. Molecular masses (in kilodaltons) are indicated.
(C) Results of yeast two-hybrid assay of self-interaction of BPH14 and the CC, NB, and CN domains.
(D) Coimmunoprecipitation assay of homocomplexes. BPH14 and the CC, NB, and CN domains were transiently expressed in rice protoplasts and analyzed by coimmunoprecipitation. Molecular masses (in kilodaltons) are indicated.
(E) BiFC visualization of self-interaction of BPH14 and the CC, NB, and CN domains in rice protoplasts. The YFP vector served as a transfected control. The DRN-CFP vector served as a nucleus marker. Confocal images of protoplasts were taken 16 to 22 h after transfection. Bars = 5 μm.

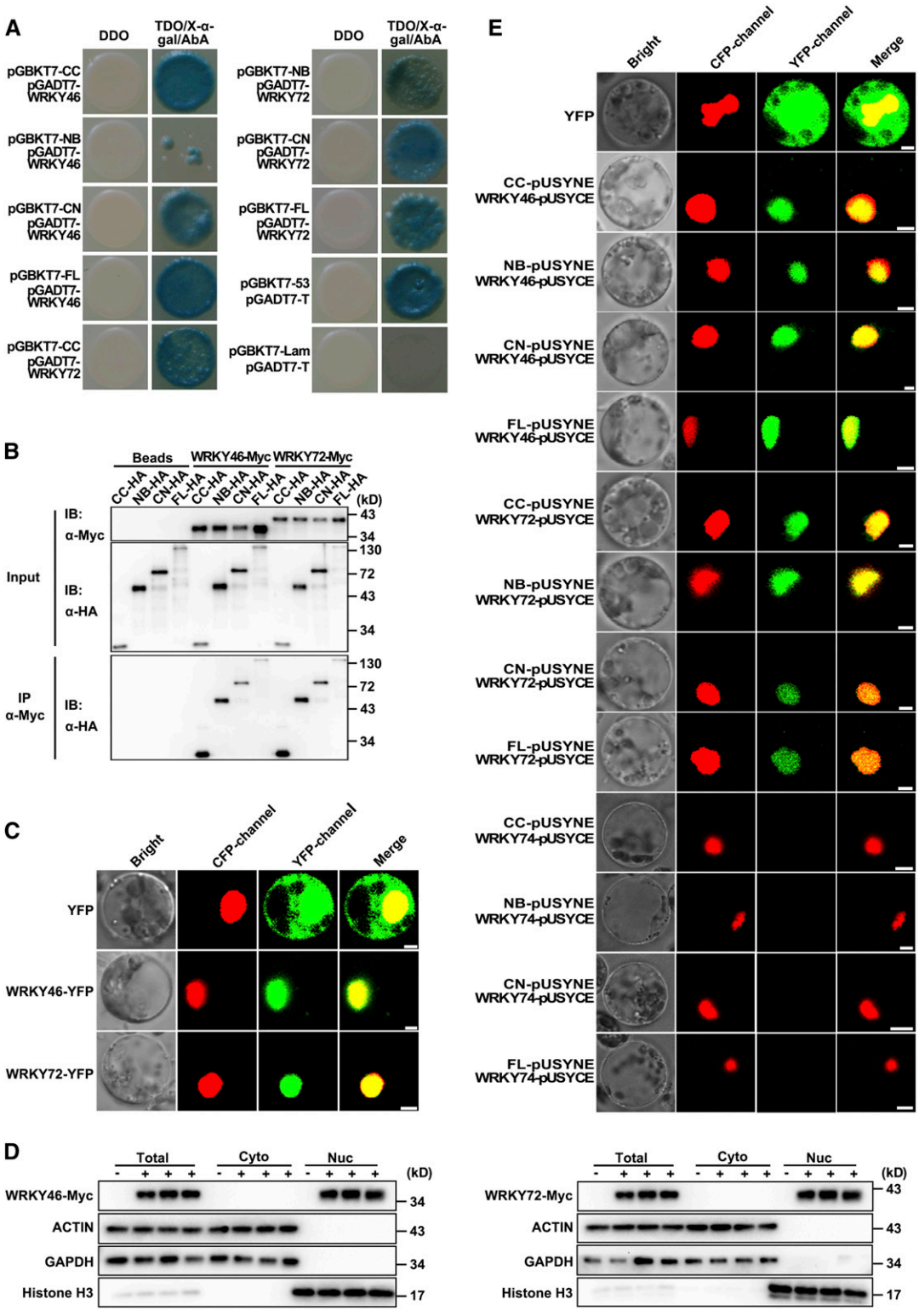

Figure 7. Transcription Factors WRKY46 and WRKY72 Interact with BPH14.

(A) Yeast two-hybrid assay of the interactions between two WRKY TFs and BPH14 or its CC, NB, or CN domains.

domains that induce the same level of resistance as the parent protein include the CC domains of MLA10 (Maekawa et al., 2011), Rp1-D21 (Wang et al., 2015a), Sr33 and Sr50 (Cesari et al., 2016), and the CN domain of RPS5 (Ade et al., 2007). NB domains have also been associated with downstream signaling leading to the activation of disease resistance in the case of the potato Rx protein (Rairdan et al., 2008) and Sw-5b (De Oliveira et al., 2016). Rairdan et al. suggested that most NB domains are innately unstable, which would explain why their ability to trigger resistance is rarely observed. However, the NB domain of BPH14 (and all of its other domains) exhibited stable protein accumulation, which may be why it induced observable resistance (Supplemental Figures 2 and 4). Our results show that a P-loop mutation (K213R) in BPH14 abolished its ability to trigger BPH resistance, indicating that nucleotide binding and hydrolysis controlled by the NB domain are critical for regulating NB-LRR protein activity and that the signaling role of the NB domain in disease and insect resistance is evolutionarily conserved. However, the CC domain of BPH14 conferred P-loop-independent BPH resistance, implying that it might mimic a postactivation state of BPH14 such that the P-loop functionality is no longer required for resistance induction. We speculate that the C-terminal LRR domain of BPH14 plays a negative regulatory role in BPH14-mediated BPH resistance, as has been reported for the LRR domains of some NB-LRR disease resistance proteins (Bai et al., 2012; Takken and Goverse, 2012; Slootweg et al., 2013). The isolated CC and NB domains do not appear to be limited by interaction with the LRR domain or nucleotide hydrolysis, which may also play a negative role in signaling activation.

Overexpressing single components of disease resistance proteins can activate the downstream defense response pathway, a phenomenon termed the "overdose effect" (Tao et al., 2000). Full-length proteins for which this is true include Rx (Bendahmane et al., 1999), RPM1 (Boyes et al., 1998), RPS2 (Tao et al., 2003), Prf (Oldroyd and Staskawicz, 1998), Sw-5b (De Oliveira et al., 2016), and RCY1 (Sato et al., 2014); this has also been observed for some single signaling component of CNLs such as MLA10 (Maekawa et al., 2011), Rp1-D21 (Wang et al., 2015a), NRG1 and ADR1 (Collier et al., 2011), Sr33 and Sr50 (Cesari et al., 2016), and RPS5, which combines two signaling components (Ade et al., 2007). We transformed the BPH-susceptible rice variety Kasalath rice with the CC domain of BPH14, the NB domain, and a construct expressing both these domains under the control of the *UBI* promoter or the native *BPH14* promoter to create overexpressing and native expression lines. All lines exhibited resistance to BPH infestation based on the same mechanism of antibiosis. These results suggest that BPH14-induced resistance is finely regulated and involves a system that is sufficiently sensitive for native expression to exceed the threshold required for the activation of downstream responses.

The CC and NB Domains Activate a Defense-Signaling Pathway

Our experiments demonstrated that the CC and NB domains activate signaling pathways in the same manner as BPH14. ROS production is a key early defense response in plant innate immunity (Boller and Felix, 2009), and rapid ROS accumulation plays a central signaling role in response to pathogen invasion (Foyer and Noctor, 2005; Mittler et al., 2011; Ge et al., 2015). In this study, the CC and NB domains, as well as the FL BPH14 protein, enhanced intracellular ROS accumulation, suggesting that ROS contribute to the BPH resistance conferred by BPH14.

SA and JA are well-established plant signaling molecules that mediate defense responses to insects (Walling, 2000; Li et al., 2006; Zarate et al., 2007; Du et al., 2009; Browse, 2009; Zhao et al., 2016). The transcript levels of SA biosynthesis-related genes accumulated more rapidly and were maintained at higher levels in CC and NB transgenic plants than in wild-type plants. This was accompanied by a similar increase in SA concentration, suggesting that endogenous SA and SA-dependent signaling pathways contributed to BPH resistance in the CC and NB transgenic lines (Figure 3). The transcript levels of JA biosynthesis-related genes increased in both transgenic and wild-type plants upon BPH infestation, and this change was accompanied by a parallel increase in JA and JA-Ile concentrations (Figure 3). These results indicate that JA signaling is involved in the basic BPH resistance response in rice.

It is well documented that plants produce and accumulate pathogenesis-related proteins (PR proteins) that are induced by biotic or abiotic stress and participate in defense responses (Sels et al., 2008). We found that the transcript levels of *PR1b*, *PR4*, *PR5*, and *PR10* increased upon BPH feeding in CC and NB transgenic plants, suggesting that the PR proteins are associated with CC-, NB-, and BPH14-induced BPH resistance (Figure 4C). Interestingly, even before BPH infestation, the CC and NB

Figure 7. (continued).

(B) Coimmunoprecipitation showing the interactions between BPH14, the CC, NB, and CN domains, and two WRKY TFs. BPH14 or the CC, NB, and CN domains and WRKY46 or WRKY72 were transiently expressed in rice protoplasts and analyzed by coimmunoprecipitation. Molecular masses (in kilodaltons) are indicated.

(C) WRKY46 and WRKY72 are localized to the nucleus in rice protoplasts. DRN-CFP was used as a nucleus marker. The YFP vector served as a transfected control. Confocal images of protoplasts were taken 16 to 22 h after transfection. Bars = 5 μm.

(D) Protein gel blot analysis of WRKY46 and WRKY72 in the cytoplasm (Cyto) and nucleus (Nuc) fraction. Nuclei-depleted and nuclei-enriched fractions were prepared from rice protoplasts and analyzed by protein gel blot analysis. Ten-fold equivalents of nuclei-enriched fractions were used relative to the nuclei-depleted fractions. WRKY46 and WRKY72 were detected in nuclei-enriched fractions using anti-Myc antibody. Histone H3 was used as a nucleus marker, and ACTIN and GAPDH as cytoplasm markers. Molecular masses (in kilodaltons) are indicated.

(E) BiFC visualization of the interactions of BPH14 or the CC, NB, and CN domains with WRKY46 or WRKY72 in transiently coexpressed rice protoplasts. The YFP vector served as a transfected control. The DRN-CFP vector served as a nucleus marker. The rice nuclear protein WRKY74 served as a BiFC negative control. Confocal images of protoplasts were taken 16 to 22 h after transfection. Bars = 5 μm.

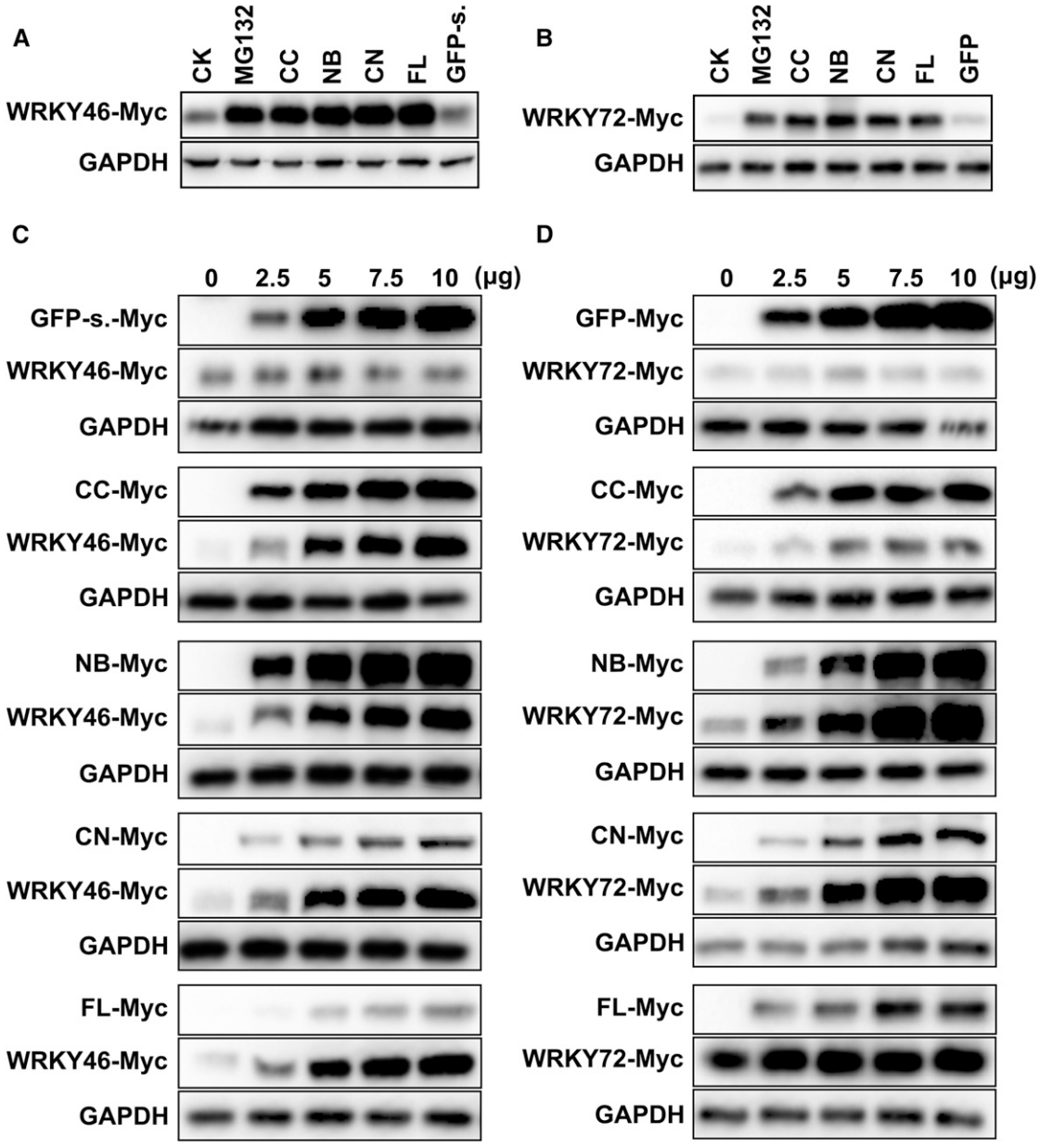

Figure 8. BPH14 Protects WRKY46 and WRKY72 Proteins from Degradation.

(A) and **(B)** Coexpression of BPH14 or the CC, NB, and CN domains enhanced WRKY46 **(A)** and WRKY72 **(B)** accumulation in rice protoplasts. WRKY46-Myc or WRKY72-Myc were translated in rice protoplasts in the absence (CK) or presence of MG132, or cotransfected with BPH14 or the CC, NB, and CN domains, and detected by protein gel blot analysis. The truncated GFP (GFP-short [GFP-s.]) or GFP served as a control. The figure is representative of three independent experiments.

(C) and **(D)** Dosage effect of BPH14 and the CC, NB, and CN domains on WRKY46 **(C)** and WRKY72 **(D)** accumulation. Rice protoplasts transfected with WRKY46-Myc **(C)** or WRKY72-Myc **(D)** were cotransfected with different amounts of CC-Myc, NB-Myc, CN-Myc, and FL-Myc. GFP-s.-Myc or GFP-Myc served as a control.

transgenic plants exhibited significantly increased ROS production, transcript levels of SA-dependent signaling pathway genes, SA levels, and transcript levels of *PR* genes relative to wild-type plants. It thus appears that their defense mechanisms were at least partially constitutively active in the absence of the LRR domain. This hypothesis is also supported by the finding that transgenic plants that were undergoing a constitutively induced defense response were in a primed state, which positively regulates plant resistance to the bacterial blight pathogen *X. oryzae.* Moreover, the primed state plays a role in reducing grain size, resulting in a large reduction in grain weight. Callose deposition on the sieve plates is an important defense mechanism that prevents

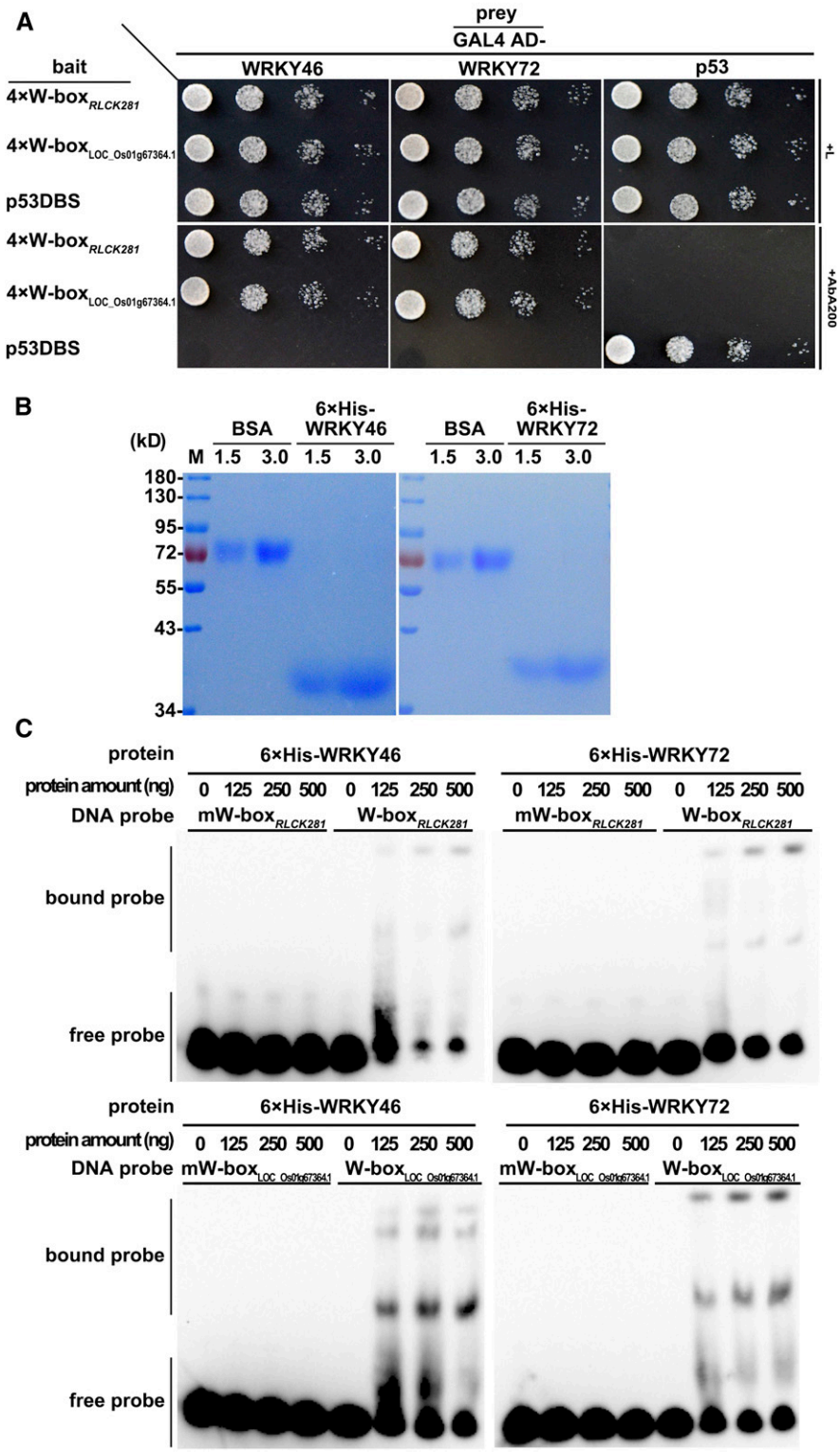

Figure 9. WRKY46 and WRKY72 Bind Specifically to W-Box$_{RLCK281}$ and W-Box$_{LOC_Os01g67364.1}$.

(A) Results of yeast one-hybrid assay showing the interactions of W-box$_{RLCK281}$ and W-box$_{LOC_Os01g67364.1}$ with WRKY46 and WRKY72. Four tandem copies of the W-box sequences (4×W-box$_{RLCK281}$ and 4×W-box$_{LOC_Os01g67364.1}$) in sense orientation were used as bait, and constructs of WRKY46 or WRKY72 fused to SV40 NLS-GAL4 AD as prey. A GAL4-AD fusion of the murine p53 protein and a bait construct containing its target sequence (p53DBS) served as controls.

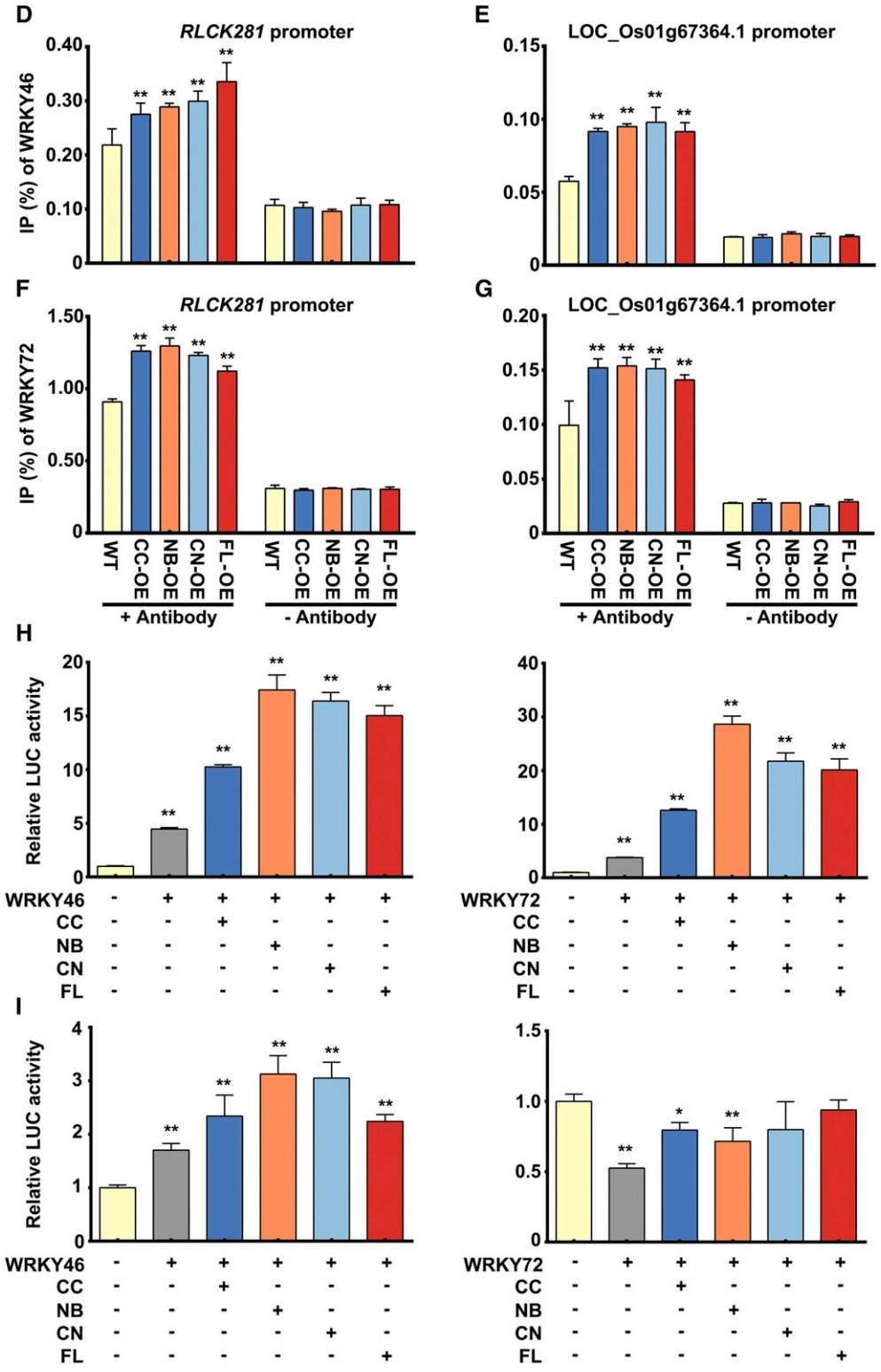

Figure 9. (Continued)

Five-microliter portions of serial dilutions of single transformants in SD liquid medium (10^{-2}, 10^{-3}, 10^{-4}, and 10^{-5}) were dropped onto SD medium containing either leucine (+L) or 200 ng/mL AbA (+AbA200). The experiment was repeated twice with similar results.

planthoppers from ingesting phloem sap (Hao et al., 2008). The CC and NB transgenic plants exhibited dramatic increases in the number of callose staining spots after BPH infestation. Taken together, these results strongly suggest that the CC and NB domains activate the same defense-signaling pathways as the full-length BPH14 protein.

BPH14 Does Not Induce HR-Like Cell Death

In the plant resistance response to pathogens, the activation of an NB-LRR gene is generally (but not always) associated with the induction of programmed cell death responses. This leads to the rapid appearance of necrotic lesions resulting from a process known as HR-like cell death, which occurs at the site of attempted pathogen invasion and is believed to limit the spread of biotrophic pathogens. However, the restriction of pathogen growth does not always correlate with cell death (Bendahmane et al., 1999; Gassmann, 2005; Coll et al., 2011; Heidrich et al., 2011). Although the transgenic plants were resistant to planthoppers, neither the isolated CC and NB domains nor the FL BPH14 protein induced hypersensitive cell death when expressed transiently in the authentic system (rice protoplasts) or an ectopic system (*N. benthamiana* leaves) (Figures 2A and 2D). Indeed, there is a growing body of evidence indicating that disease resistance and HR-related programmed cell death are distinct processes. Support for this hypothesis comes from studies on Rx (Slootweg et al., 2010), RPS4 (Heidrich et al., 2011), and N (Bhattacharjee et al., 2009). Moreover, cell death appears to be uncoupled from the defense mechanisms induced by plant disease resistance genes encoding R proteins such as Rdg2a (Bulgarelli et al., 2010), Rrs1 (Lehnackers and Knogge, 1990), Mla1 (Freialdenhoven et al., 1994), Rx (Bendahmane et al., 1999), RPS4, RPS6 (Gassmann, 2005), and Mi-1 (Martinez de Ilarduya et al., 2003). These findings indicate that plant immunity can be effective without programmed host cell death.

BPH is a monophagous herbivore that sucks the phloem sap of rice plants through its stylet mouthparts with a moving feeding style, which is very different from pathogen infection that is localized to a specific area of the plant. HR-like cell death restricts pathogen growth and confers some level of local resistance, but this strategy is wholly ineffective against a mobile organism such as BPH that can simply move to another part of the plant (Kombrink and Schmelzer, 2001). The *Rx* gene in potato is thought to very rapidly induce extreme resistance to potato virus X, preventing the avirulence factor from accumulating to a degree that would otherwise trigger a more extensive host response (Bendahmane et al., 1999). BPH14 induces antibiosis but not antixenosis resistance to planthoppers, suggesting that the elicitation of extreme resistance (unlike that of HR) occurs rapidly and independently of HR, making it an efficient disease resistance mechanism (Künstler et al., 2016). A rapid oxidative burst appears to play a role in HR-independent extreme resistance, enabling a rapid and usually symptomless process that eliminates pathogens promptly without overly stressing the plant's resource reserves (Figure 4A; Supplemental Figure 8) (Hafez and Kiraly, 2003; Bacsó et al., 2011). We also propose that inducible responses giving rise to physical and chemical barriers to BPH infection in the cell walls (such as callose deposition) and intercellular spaces of the rice plant represent mechanisms by which BPH14 mediates resistance to BPH infestation without inducing hypersensitive cell death (Figure 4B; Supplemental Figure 9).

Figure 9. (continued).

(B) Purified 6×His-WRKY46 and 6×His-WRKY72 proteins used in the EMSA. Protein concentrations were determined by the Bradford assay. Portions (1.5 and 3.0 μg) of purified 6×His-WRKY46, 6×His-WRKY72, and BSA were separated in a 10% SDS polyacrylamide gel and stained with Coomassie brilliant blue. Molecular masses (in kilodaltons) are indicated.

(C) EMSA showing that WRKY46 and WRKY72 bound specifically to the W-box$_{RLCK281}$ and W-box$_{LOC_Os01g67364.1}$ probes. Positions of bound and free DNA probes are indicated on the left. Note that along with differences in amounts (in nanograms) of proteins to DNA probes, the gradually increasing band shifts with W-box$_{RLCK281}$ (upper panel) and W-box$_{LOC_Os01g67364.1}$ (lower panel) probes but not mutant probes (mW-box$_{RLCK281}$ and mW-box$_{LOC_Os01g67364.1}$), indicating that WRKY46 and WRKY72 bind specifically to the W-box$_{RLCK281}$ and W-box$_{LOC_Os01g67364.1}$ probes, respectively. Each EMSA experiment was repeated three times with similar results.

(D) to **(G)** WRKY46 and WRKY72 proteins bound to the promoter regions of *RLCK281* (**[D]** and **[F]**) and LOC_Os01g67364.1 (**[E]** and **[G]**) analyzed by ChIP assay. Rice protoplast samples were prepared using wild-type Kasalath (WT) and transgenic plants (CC-OE, NB-OE, CN-OE, and FL-OE), which were transfected with WRKY46-Myc (**[D]** and **[E]**) or WRKY72-Myc (**[F]** and **[G]**). The qPCR was conducted before immunoprecipitation (input), after IP with anti-Myc antibody (+ Antibody), or after IP without anti-Myc antibody (− Antibody). The presented percentage of PCR product from IP is relative (IP/input %) to that from input. Data represent the means (three biologically independent experiments for PCR products from IP) ± SD. The PCR products from IP with anti-Myc antibody all significantly differ from the PCR products from IP without anti-Myc antibody in wild-type and transgenic protoplast samples. Data were subjected to ANOVA as detailed in Methods, and asterisks indicate a significant difference between the PCR products from IP with anti-Myc antibody in wild-type and transgenic protoplast samples expressing the WRKY46 and WRKY72 proteins (*$P \leq 0.05$; **$P \leq 0.01$). OE, homozygous (T3 generation) overexpressing transgenic lines.

(H) and **(I)** Transactivation assay showing enhancement of *RLCK281* and LOC_Os01g67364.1 transcription by BPH14 and the CC, NB, and CN domains. The reporter construct contained putative promoter sequences (2 kb upstream of the translational start codon) of *RLCK281* **(H)** and LOC_Os01g67364.1 **(I)**. The reporter, *WRKY46* or *WRKY72*, and reference (*Pro35S:RLUC*) plasmids were delivered into rice protoplasts using the PEG method, in the absence or cotranslated with *BPH14* or the *CC*, *NB*, and *CN* domains. LUC reporter activity was determined and normalized to an internal *Pro35S:RLUC* control. The results represent the means (eight technical replicates from one biological experiment) ± SD. Data were subjected to ANOVA as detailed in Methods, and asterisks indicate significant differences of the transcriptional activities between the protoplasts transformed with the *WRKY46* or *WRKY72*, in the absence or cotranslated with *BPH14* or the *CC*, *NB*, and *CN* domains and the reporter only (*$P \leq 0.05$; **$P \leq 0.01$). Three biologically independent experiments were performed, yielding equivalent results.

The Oligomerization of BPH14 Is Implicated in Plant Immunity

Previous studies on plant proteins such as the CNL receptor Prf (Gutierrez et al., 2010; Ntoukakis et al., 2014) and RPS5 (Ade et al., 2007) have suggested that oligomerization of plant NLRs plays some type of role in the activation of defense mechanisms. Crystallographic analyses of the structures and functions of the N-terminal domains of MLA10 confirmed that they form homodimers and revealed the nature of the interface for each N-terminal dimer module. Like MLA10, the NMR structure of the wheat Sr33 protein, an ortholog of MLA, was also solved and found to form dimers in solution. These examples suggest that self-association is critical for signaling involving CNLs (Maekawa et al., 2011; Casey et al., 2016). A similar mechanism has been demonstrated in more extensive studies of animal NLRs. For example, upon recognition of invading pathogens or danger signals, an activated NAIP2 molecule provides a platform for self-oligomerization of NLRC4 monomer to form a wheel-shaped oligomer called the inflammasome, in which NLRC4 recruits caspase-1 directly through CARD-CARD interactions and transduces the immune signal (Hu et al., 2015; Zhang et al., 2015; Lu et al., 2016). Apaf-1, CED-4, and human NOD proteins also form oligomers via NB-ARC-mediated interactions, which may or may not be accompanied by dimerization of the N-terminal domains in vertebrate proteins. Conversely, plant NLRs lack the ARC3 subdomain within the NB-ARC domain, which appears to be critical for the oligomerization of animal NLRs (Proell et al., 2008; Danot et al., 2009; Qi et al., 2010; von Moltke et al., 2013). Among plant NLRs, to date, only the RPS5 NB domain has been shown to self-associate, and overexpression of a CC-NB construct of this protein induced cell death (Ade et al., 2007). Overexpression of the isolated NB domains of Rx and Sw-5b also induced cell death (Rairdan et al., 2008; De Oliveira et al., 2016). Here, we show that the BPH14 protein and its isolated CC and NB domains can self-associate in vivo (Figures 6C to 6E). However, our data do not clearly distinguish between dimerization and higher-order oligomerization. It is therefore possible that higher-order complexes form after the initial dimerization event, potentially giving rise to high molecular weight complexes reminiscent of animal inflammasomes (Vanaja et al., 2015).

Notably, the powdery mildew resistance receptor, i.e., the CNL Pm8 derived from rye (*Secale cereale*), can form self-association complexes with its ortholog Pm3 or with different allelic forms of Pm3 in wheat (Brunner et al., 2011; Stirnweis et al., 2014). Since phylogenetic analysis has shown that BPH14 is more closely related to Pm8 than to most other known plant disease resistance proteins, studies on Pm8 and its ortholog Pm3 may provide some insight into its behavior. Together with our data on BPH14, this suggests that BPH14 may work by itself or in conjunction with orthologs to engage downstream signaling components. These mechanistic diversities and complexities could be elucidated by mutation analysis or crystallographic studies in the future.

Downstream Signal Transduction and Defense Mechanism Activation by BPH14

There are some reports of activated NLRs binding to signaling proteins and directly influencing transcriptional regulation in plants. For example, the R protein SNC1 binds to TPR1 and the transcription factor bHLH84 (Zhu et al., 2010; Xu et al., 2014), N binds to the transcription factor SPL6 (Padmanabhan et al., 2013), and RPS4 binds to the ribosome biogenesis regulator homolog RRS1 (Williams et al., 2014). Interactions between NLRs and WRKY TFs, which are involved in defense signal transduction, have also been reported in plants. For example, MLA10 interacts with HvWRKY1 and HvMYB6 (Shen et al., 2007; Chang et al., 2013), Pb1 interacts with WRKY45 (Inoue et al., 2013; Matsushita et al., 2013), and Xa21 interacts with WRKY62 (Peng et al., 2008; Park and Ronald, 2012). We observed that the transcript levels of *WRKY46* and *WRKY72* differed, suggesting that WRKY72 may be directly involved in the defense response signaling pathway while WRKY46 contributes in some other way (Supplemental Figure 13). Previous data imply that WRKY46 and WRKY72 function in disease resistance signaling. *WRKY46* transcript levels were significantly repressed following plant inoculation with avirulent *M. oryzae* strain CL3.6.7 (Abbruscato et al., 2012), while *WRKY72* transcript levels were highly upregulated in 9804 (a japonica rice variety, which was used as the recipient of the maize *Rxo1* gene) after inoculation with the bacterial

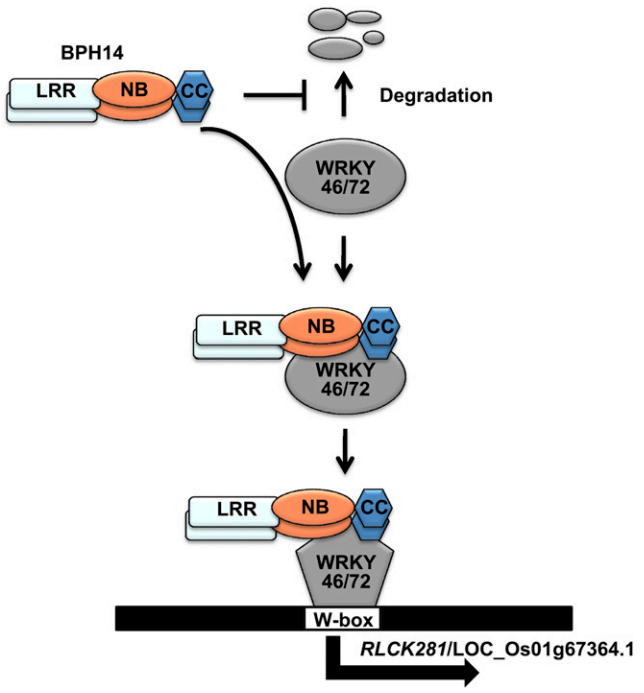

Figure 10. Proposed Model for the Interaction of BPH14 with WRKY46 and WRKY72 and the Initiation of Defense Signaling.

The BPH14 monomers are assembled into a homodimer, which is capable of interacting with WRKY46 and WRKY72. Coexpression of BPH14 is considered to protect WRKY46 and WRKY72 from degradation by the ubiquitin proteasome system. The dimer formed from BPH14 can directly interact with WRKY46 and WRKY72, thereby enhancing its W-box binding activity and potentiating defense gene (e.g., *RLCK281* or LOC_Os01g67364.1) expression and immune responses. WRKY46 and WRKY72 are shown as pentagons representing the conformation whose DNA binding activity is enhanced by binding of the dimer formed by BPH14.

pathogen, *X. oryzae* pv *oryzicola* (Zhou et al., 2010). WRKY72 protein was also specifically phosphorylated after 24 h of *X. oryzae* pv *oryzae* infection (Hou et al., 2015). We found that the BPH14 protein and its CC, NB, and CN domains interacted with WRKY46 and WRKY72, protecting them from UPS degradation. We speculate that this stabilization of WRKY46 and WRKY72 increases their transcriptional activity or that UPS-dependent WRKY46 and WRKY72 degradation represses the defense mechanism.

We designed more sophisticated ChIP experiments to identify the target genes of WRKY46 and WRKY72 to facilitate the analysis of their functions. Yeast one-hybrid screening and EMSA experiments revealed that the W-box elements of *RLCK281* and LOC_Os01g67364.1 interact with WRKY46 and WRKY72, respectively. Several RLCKs are thought to play pivotal roles in plant defense (Martin et al., 1994; Swiderski and Innes, 2001; Zhang et al., 2010; Shi et al., 2013; Liu et al., 2011; Feng et al., 2012; Shinya et al., 2014; Yamaguchi et al., 2013; Dubouzet et al., 2011; Wang et al., 2015b; Zhou et al., 2016) and are thought to be involved in connecting signal perception by RLKs in the plasma membrane to downstream intracellular signal transduction systems. Callose synthases such as LOC_Os01g67364.1 perform callose biosynthesis in plants (Xie et al., 2011), and there is considerable evidence that they function in preventing penetration by herbivores (Enrique et al., 2011; Blümke et al., 2013, 2014; Ellinger et al., 2013). We found that the promoters of *RLCK281* and LOC_Os01g67364.1 were associated with WRKY46 and WRKY72; the presence of the CC, NB, and CN domains or FL BPH14 enhanced the association between the WRKYs and the promoters of *RLCK281* and LOC_Os01g67364.1 in rice. The transactivation activities of these genes were regulated by these two TFs, with or without the CC, NB, and CN domains or FL BPH14. We therefore suggest that BPH14 is involved in the transcription of some *RLCKs* (e.g., *RLCK281*) and some callose synthase genes (e.g., LOC_Os01g67364.1) via its interactions with WRKY46 and WRKY72 and that these TFs may mediate the defense responses of rice to BPH attack.

In conclusion, we demonstrated that BPH14 and the isolated CC, NB, or CN domains confer resistance to BPH infestation by activating the SA signaling pathway. Interestingly, a recent study reported that PATTERN-TRIGGERED IMMUNITY COMPROMISED RECEPTOR-LIKE CYTOPLASMIC KINASE1 (PCRK1) and PCRK2 regulate SA biosynthesis by influencing the expression of two transcription factors, *SAR DEFICIENT1* (*SARD1*) and *CALMODULIN BINDING PROTEIN 60-LIKE.g* (*CBP60g*), in Arabidopsis (Kong et al., 2016). Moreover, in rice, PBL1 protein facilitates the activation of the SA-dependent pathway in the defense response against pathogen attack (Khare et al., 2016). Further studies will be needed to determine whether RLCK281 is involved in regulating SA signaling. Additionally, studies on phytohormone defense signaling have shown that SA treatment can affect callose synthase gene expression (Jacobs et al., 2003; Dong et al., 2008). We propose that LOC_Os01g67364.1 may function as part of a callose synthase and contribute to callose accumulation to protect plants against BPH attack. As such, it would be interesting to determine whether its expression correlates positively with SA levels.

Proposed Model for the Interaction of BPH14 with WRKY46 and WRKY72 and the Initiation of Defense Signaling

We observed the self-association of BPH14 and its interactions with WRKY46 and WRKY72. In addition, we obtained useful information concerning the relationship between the activation of BPH resistance and the induction of signaling. Based on these results, we developed a model of the key protein-protein and protein-DNA interactions that function in BPH14-mediated immune responses, which is shown in Figure 10. Our model suggests that BPH14 or its CC, NB, or CN domains form dimeric structures and recruit signaling partners including WRKY46 and WRKY72. However, with the exception of *RLCK281* and LOC_Os01g67364.1, the downstream signaling partners activated in this process remain unknown. Identifying these genes will greatly increase our knowledge of plant resistance to insects.

METHODS

Plant Materials

The *indica* rice (*Oryza sativa*) variety Kasalath, which is susceptible to attack by BPH (*Nilaparvata lugens*), was grown during the normal rice growing seasons under natural field conditions at the Genetics Institute at Wuhan University and was used as the transgenic acceptor and as a susceptible rice control. *Nicotiana benthamiana* plants were grown in a growth chamber at 22°C under high-pressure sodium lamps (200 to 300 μmol s^{-1} m^{-2} light) with a 16-h-light/8-h-dark photoperiod.

Insect Population Maintenance and BPH Resistance Evaluation

The BPH insects used for infestation were maintained on the susceptible cultivar Taichung Native 1 (TN1) at Wuhan University, China. Approximately 15 seeds harvested from each T2 individual transformant or Kasalath were sown in a 9-cm-diameter plastic pot. At the four-leaf stage, the seedlings were infested with second to third instar BPH nymphs at a rate of eight insects per seedling. Once all seedlings of the susceptible control were dead, the plants were examined and each seedling was assigned a score as described by Huang et al. (2001). At least three replicates were used for each cultivar or line.

Host Choice Test

In the host choice test, four-leaf stage rice plants were grown in a single plastic bucket. Two of the plants in each bucket were Kasalath, and the other two were from one of the transgenic lines. Plants from the same line were placed in opposition to each other. Forty third-instar BPH nymphs were then placed in the buckets, and the number of nymphs that settled on each plant was recorded at 3, 6, 24, 48, and 72 h after release. Ten buckets were analyzed for each transgenic line included in the study.

Honeydew Excretion and BPH Weight Gain Measurements

A total of 30 third-instar BPH nymphs previously starved for 2 h were weighed and confined to a preweighed Parafilm sachet attached to the leaf sheath of a rice plant (Pathak et al., 1982). After 2 d of feeding, the sachets were removed from the plants and the insects were removed from the sachets. Both the insects and the honeydew in each sachet were weighed again, and the weight difference of the Parafilm sachet was recorded as the honeydew excretion. The change in the insects' weight was recorded as the BPH weight gain.

Bacterial and Fungal Pathogen Inoculation

To examine bacterial blight disease resistance, wild-type and transgenic rice plants at the four-leaf stage were inoculated with the bacterial pathogen *Xanthomonas oryzae* (strain PXO99) using the leaf-clipping method (Chen et al., 2002). The inoculated plants were grown and examined under natural field conditions during the normal rice growing season from June to August at the Experimental Station of Wuhan University, Wuhan, China. Disease severity was scored by measuring the percentage of the lesion area (lesion length/leaf length) at 10 d after inoculation.

To evaluate fungal blast disease resistance, wild-type and transgenic rice plants at the four-leaf stage were inoculated with the fungal pathogen *Magnaporthe oryzae* (strain M13Ac007) by spray inoculation (Chen et al., 2003). The inoculated plants were grown in a growth chamber at 28°C in darkness for 24 h and then under a 16-h-light/8-h-dark cycle with 95% humidity. Disease severity was scored for individual plants at 6 d after inoculation, and the disease severity score was given following the standard evaluation system developed by the International Rice Research Institute, where a score of 0 indicates no lesions and a score of 9 represents more than 75% of leaf area affected (International Rice Research Institute, 2002).

Gene Constructs

Routine molecular cloning techniques were used to prepare the constructs. The gene constructs and primers used in this work are listed in Supplemental Data Sets 4 and 5. All of the resulting recombinant vectors were sequenced.

ZeBaTA-based expression vectors for gene overexpression, designated pCXUN-4×HA and pCXUN-4×Myc, were created by adding a C-terminal 4×HA or 4×Myc tag to the pCXUN vector (Chen et al., 2009). ZeBaTA-based expression vectors for native gene expression, designated Rap-4×Myc, were derived from pCXUN-4×Myc by replacing the *UBI* promoter with the native *BPH14* (*Ra*) promoter via *Hind*III and *Bam*HI digestion and ligation.

The *CC*, *NB*, *LRR*, *CN*, *NL*, and *CL* fragments, the P-loop (K213R) mutant *KR*, and *FL BPH14* were amplified from B5 cDNA and cloned into the vector pCXUN-4×HA, while the *CC*, *NB*, and *CN* fragments and *FL BPH14* were amplified from B5 cDNA and cloned into the vector Rap-4×Myc using the TA cloning system (Chen et al., 2009). The P-loop (K213R) mutant *KR* and *CL* fragments were generated by overlap extension PCR (Ho et al., 1989; Horton et al., 1989) using two sets of primer pairs (Supplemental Data Set 4), with FL-HA as the template. The two resulting PCR products were joined in a second amplification step using the primer pairs RaK213R-F/RaK213R-R and LRRPJ-F/CCPJ-R (Supplemental Data Set 5). These constructs were used for *Agrobacterium tumefaciens*-mediated transformation of Kasalath rice.

Constructs used for rice protoplast transfection and *N. benthamiana* agroinfiltration experiments were generated with pCXUN-4×HA and pCXUN-4×Myc. The coding sequences for the *CC*, *NB*, and *CN* domains, and *FL BPH14*, were cloned into pCXUN-4×HA, yielding vectors designated CC-HA, NB-HA, CN-HA, and FL-HA, respectively. Additionally, the coding sequences for the *CC*, *NB*, and *CN* domains, *FL BPH14*, *GFP*, truncated *GFP* (*GFP-short*), *WRKY46*, and *WRKY72* were cloned into pCXUN-4×Myc, yielding vectors designated CC-Myc, NB-Myc, CN-Myc and FL-Myc, GFP-Myc, GFP-short-Myc, WRKY46-Myc, and WRKY72-Myc, respectively.

A *YFP* fragment was amplified by PCR using a left primer with *Avr*II and *Spe*I sites and cloned into the vector pCXUN-4×Myc to obtain the pCXUN-YFP-4×Myc fusion construct. To analyze the subcellular localization of the *CC*, *NB*, and *CN* domains, *FL BPH14*, *WRKY46*, and *WRKY72*, their coding sequences were cloned in-frame into the *Avr*II and *Spe*I sites of C-terminal *YFP*, respectively, using the pCXUN-YFP-4×Myc vector.

For BiFC analysis, the *35S* promoters of the pSPYNE vector and the pSPYCE vector (Walter et al., 2004) were replaced by the *UBI* promoters using the *Hind*III and *Xma*I sites to obtain the pUSYNE vector and the pUSYCE vector, respectively. The coding sequences for the *CC*, *NB*, and *CN* domains, and *FL BPH14*, were cloned in-frame into the *Xma*I site of the pUSYNE vector. The coding sequence of the *CC*, *NB*, and *CN* domain and *FL BPH14*, *WRKY46*, *WRKY72*, and *WRKY74* were cloned in-frame into the *Xma*I site of the pUSYCE vector.

For yeast two-hybrid analysis, the coding sequences of the *CC*, *NB*, and *CN* domains and *FL BPH14* and *WRKY46* and *WRKY72* were separately cloned in-frame into the *Nde*I and *Eco*RI sites of the pGBKT7 and pGADT7 vectors, yielding vectors designated pGBKT7-CC, pGBKT7-NB, pGBKT7-CN, pGBKT7-FL, pGADT7-CC, pGADT7-NB, pGADT7-CN, pGADT7-FL, pGADT7-WRKY46, and pGADT7-WRKY72.

For yeast one-hybrid analysis, four copies of the bait DNA sequence (W-box) in tandem were cloned in-frame into the *Hind*III and *Xho*I sites of the pAbAi vector to yield bait constructs designated pAbAi-4×W-box$_{RLCK281}$ and pAbAi-4×W-box$_{LOC_Os01g67364.1}$. The pGADT7-WRKY46 and pGADT7-WRKY72 constructs were used as prey.

For expression and purification of proteins used in the EMSA, the coding sequences of *WRKY46* and *WRKY72* were cloned into the *Eco*RI and *Xho*I sites of the pET-28a expression vector (EMD Biosciences, Novagen), yielding constructs designated 6×His-WRKY46 and 6×His-WRKY72, respectively.

Constructs for the split luciferase assay were generated by modifying the FRK1-LUC vector construct (Zhang et al., 2010). The reporter plasmids *Pro*$_{RLCK281}$-LUC and *Pro*$_{LOC\_Os01g67364.1}$-LUC were generated by replacing the *FRK1* sequence in the FRK1-LUC vector with the putative promoter sequences (2 kb upstream of the translational start codon) of *RLCK281* and LOC_Os01g67364.1 using the *Nde*I and *Xho*I sites or *Nde*I and *Kpn*I sites, respectively.

Generation of Transgenic Rice Plants

Overexpression and native expression constructs of *BPH14* and its isolated domains were transformed into Kasalath rice using an Agrobacterium-mediated method (Nishimura et al., 2005). T0 transgenic plants were grown in a greenhouse under a 14-h-light/10-h-dark cycle at 28°C.

Phenotypic Evaluation

To measure grain traits, harvested rice grains were air-dried and stored at −20°C prior to testing. Ten randomly chosen, filled grains from each plant were lined up lengthwise along a vernier caliper to measure grain length and then arranged by breadth and thickness to measure grain width and grain thickness. The measurement was performed five times for each plant, and each replicate was performed using 10 different grains. The 1000-grain weight was calculated based on 100 grains and converted to 1000-grain weight, the measurement was performed in triplicate for each plant, and each replicate was performed using 100 different grains.

For seed germination measurements, 50 seeds of each tested line were imbibed in tap water at 28°C for 5 d and transferred to Petri dishes containing water-saturated filter paper to germinate. Germination rates were scored 3 d after transfer to dishes. Seeds were regarded as having germinated when the radicle was longer than 1 mm. The test was performed in triplicate, and each biological replicate was performed using 50 such seeds.

To measure 7-d-old seminal root length, the germinated seeds were transferred to plastic nets that were installed on the upper surfaces of plastic boxes that contained just enough distilled water to maintain contact with the germinated seeds. The boxes were placed in a plant growth chamber at 28°C for 7 d for seminal root growth. The length of each 7-d-old seminal root was measured from the seed surface to the tip of the longest root.

For plant morphological characterization, plant height, the length of the fourth leaf (from the base leaf of the plant), and the width of the fourth leaf were measured in rice seedlings at the four-leaf stage rice. Plant height was measured from the soil surface to the tip of the tallest leaf. The length and width of the fourth leaf were measured at the longest and widest part of the leaf blade.

Protein Extraction, Protein Gel Blot Analysis, and Coimmunoprecipitation

Proteins from transgenic rice plants were extracted from the leaf sheaths of 15-d-old seedling tissue for immunoblotting as described previously (Hu et al., 2011). Fusion proteins were detected using an anti-HA antibody (MBL; catalog no. M180-3) or an anti-Myc antibody (MBL; catalog no. M192-3) at a dilution ratio of 1:1000 with dilution buffer (20 mM Tris-HCl, pH 7.4, 150 mM NaCl, 0.1% [w/v] Tween 20, and 3% [w/v] BSA), followed by a subsequent incubation with 1:10,000 diluted secondary antibody conjugated to horseradish peroxidase (Jackson; catalog no. 115-035-003) with 5% (w/v) skimmed milk.

Protein extracts from *N. benthamiana* leaves were prepared as described below. Leaf samples were collected 48 h after agroinfiltration. Total soluble proteins from three 11-mm-diameter leaf discs taken from the infiltrated area were extracted in 200 μL of 2× Laemmli buffer (Laemmli, 1970), boiled, and centrifuged. Proteins from 10 μL of the resulting supernatant were separated via SDS-PAGE, and the Myc-tagged protein fraction was detected by immunoblotting using an anti-Myc antibody (MBL; catalog no. M192-3) at a dilution ratio of 1:1000 with dilution buffer (20 mM Tris-HCl, pH 7.4, 150 mM NaCl, 0.1% [w/v] Tween 20, and 3% [w/v] BSA), followed by a subsequent incubation with 1:10,000 diluted secondary antibody conjugated to horseradish peroxidase (Jackson; catalog no. 115-035-003) with 5% (w/v) skimmed milk.

Protein extracts from rice protoplasts were prepared in rice protein extraction buffer consisting of 100 mM Tris-HCl (pH 7.5), 1 mM EDTA, 5 mM $MgCl_2$, and 0.5% (w/v) Triton X-100, with 2 mM DTT and 1 mM PMSF added immediately before use. Total soluble proteins from rice protoplast samples comprising ~5 × 10^6 cells each were extracted in 200 μL of rice protoplast protein extraction buffer. Ten microliters of the extract was then separated by SDS-PAGE and subjected to immunoblotting using an anti-HA antibody (MBL; catalog no. M180-3) or an anti-Myc antibody (MBL; catalog no. M192-3) at a dilution ratio of 1:1000 with dilution buffer (20 mM Tris-HCl, pH 7.4, 150 mM NaCl, 0.1% [w/v] Tween 20, and 3% [w/v] BSA), followed by a subsequent incubation with 1:10,000 diluted secondary antibody conjugated to horseradish peroxidase (Jackson; catalog no. 115-035-003) with 5% (w/v) skim milk. The Tanon high-sig ECL protein gel blotting substrate was used for detection.

For rice protoplast coimmunoprecipitation assays, the CC-Myc, NB-Myc, CN-Myc, and FL-Myc constructs were coexpressed with CC-HA, NB-HA, CN-HA, FL-HA, WRKY46-Myc, and WRKY72-Myc in rice protoplasts. The protoplasts were incubated for 16 to 22 h after transfection, after which total proteins were extracted with rice protein extraction buffer. For anti-Myc IP, total proteins were precleared with protein G agarose (Roche) for 1 h, followed by precipitation with 2 μg anti-Myc antibody (MBL; M192-3) together with protein G agarose for 4 h at 4°C. The coimmunoprecipitated proteins were analyzed by SDS-PAGE. Immunoblot analysis was performed using anti-Myc-tag mAb-HRP-DirecT (MBL; catalog no. M192-7) or anti-HA-tag mAb-HRP-DirecT (MBL; catalog no. M180-7) antibodies at a dilution ratio of 1:1000 with dilution buffer (20 mM Tris-HCl, pH 7.4, 150 mM NaCl, 0.1% [w/v] Tween 20, and 3% [w/v] BSA), respectively.

First-Strand cDNA Synthesis and qRT-PCR Analysis

Seeds from wild-type plants and transgenic plants expressing one of the *CC*, *NB*, and *CN* domains or *FL BPH14* were sown in 9-cm-diameter plastic cups. At the four-leaf stage, plants were infested with eight second-instar nymphs per plant and sampled after 0, 3, 6, 12, 24, 48, and 72 h. All treatments, each with three biological replicates, with each biological replicate having 15 seedlings per rice line used for analysis, were terminated at the same time. Total RNA was extracted from the leaf sheaths and converted into first-strand cDNA using an oligo(dT) primer and random 6-mers from a PrimeScript RT reagent kit with gDNA Eraser (Takara; code no. RR047Q), according to the manufacturer's instructions, using 3 μg of total RNA from each sample for reverse transcription. The cDNA was diluted 10-fold and amplified for qRT-PCR analysis. The expression of selected genes was quantified by qRT-PCR using a C1000 Touch Thermal Cycler (Bio-Rad) and the primers listed in Supplemental Data Set 6. Expression was evaluated by relative quantification (Livak and Schmittgen, 2001).

Transient Protein Expression and Cell Death Assays in *N. benthamiana*

Agrobacteria-mediated transient expression (agroinfiltration) was performed using the Agrobacterium strain GV3101 carrying the indicated constructs, which was grown in Luria-Bertani liquid medium containing 50 mg/mL rifampicin, 15 mg/mL gentamycin, and 25 mg/mL kanamycin at 28°C for 24 h. Bacteria were harvested by centrifugation, resuspended in infiltration medium (10 mM MES pH 5.6, 10 mM $MgCl_2$, and 150 μM acetosyringone), grown to an OD_{600} of 0.5, and incubated for 2 h at room temperature before leaf infiltration. The 4- to 5-week-old infiltrated plants were incubated in growth chambers under controlled conditions at 22°C with a 16-h-light period for the cell death assays.

Rice Protoplast Viability Assays

Rice protoplasts were prepared as described previously using normal green rice seedlings instead of etiolated rice seedlings of the Nipponbare cultivar (Chen et al., 2006). The *Pro35S:RLUC* (Renilla luciferase) was used as a reporter to monitor protoplast viability (Zhang et al., 2010). Specified combinations of constructs were cotransfected together with the *Pro35S:RLUC* plasmid into rice protoplasts using the PEG method (Chen et al., 2006). Luciferase activity was measured 16 to 22 h after transfection using a luciferase assay system (Promega), and the reduction in luminescence was compared with that for a control comprising empty vector-transfected protoplasts.

ROS Measurements

For histochemical detection of ROS in rice protoplasts, rice protoplasts were prepared enzymatically as described above (Chen et al., 2006). After transfection for 16 to 22 h, the protoplasts were resuspended in W1 solution (0.5 M mannitol, 4 mM MES, pH 5.7, and 20 mM KCl) after rinsing with W5 (154 mM NaCl, 125 mM $CaCl_2$, 5 mM KCl, and 2 mM MES, pH 5.7) and allowed to sit and recover for 5 h before treatment. After resting, the protoplasts were quantified with a hemocytometer and aliquoted into a 24-well Corning Costar cell culture plate, where they were diluted in W1 to a concentration of 1 × 10^5 cells/200 μL. The cell culture plate was then moved to a light bank where the protoplasts were left under bright light (100 to 150 μmol s^{-1} m^{-2} light) for 1 h. Prior to imaging, 750 nM H_2DCFDA (CalBioChem) was added and the cells were incubated in darkness for 12 to 15 min. Images used for quantification (as shown in Figure 4A) were obtained using a Leica (TCS SP8) epifluorescent microscope with a GFP cube. Fluorescence was quantified using ImageJ from a minimum of 25 protoplasts across 10 or more images per genotype (Henry et al., 2015).

Hydrogen peroxide contents were determined by the chemiluminescence method based on the Co (II)-catalyzed oxidation of luminol as previously described (Pérez and Rubio, 2006). Transfected rice protoplasts

for histochemical ROS detection were prepared as described above. At 16 to 22 h after transfection, the protoplasts were quantified and diluted with W5 to 1×10^5 cells/200 μL. Horseradish peroxidase (20 μg/mL; Sigma-Aldrich) and 21 nM of the luminol derivative 8-amino-5-chloro-7-phenylpyrido [3,4-d] pyridazine-1,4 (2H,3H) dione (L-012) (Wako) were added to the protoplasts before the start of the experiment (Nishinaka et al., 1993). In addition, crab shell chitin (200 μg/mL) was added to the prepared protoplasts to serve as a positive control. Luminescence was captured using a Photek camera system and analyzed using software supplied by the manufacturer and Microsoft Office Excel. At least three independent experiments measuring hydrogen peroxide contents were performed, with similar results on different days.

Simultaneous Quantification of Multiple Phytohormones (SA and JA) and Hormone Metabolites (JA-Ile)

JA and SA standards were purchased from Sigma-Aldrich, and JA-Ile was obtained from OlChemIm. The internal standards were 10-dihydro-JA (OlChemIm) for JA and JA-Ile and naphthaleneacetic acid (OlChemIm) for SA.

To estimate endogenous SA, JA, and JA-Ile levels, three replicates of each frozen leaf sheath sample (~100 mg for each replicate) were ground to a fine power in liquid nitrogen using a mortar and pestle. Each sample was then homogenized in 750 μL cold extraction buffer (methanol:water:acetic acid, 80:19:1, v/v/v) supplemented with internal standards, 10 ng 10-dihydro-JA, and 3 μg naphthaleneacetic acid and shaken at 4°C overnight. The subsequent extraction procedure was performed according to a previous report (Liu et al., 2012), and the extracts were filtered through a 0.22-μm nylon membrane and dried by evaporation under a flow of nitrogen gas for ~4 h at room temperature before being dissolved in 200 μL methanol. The samples were stored at −70°C until use. The quantification of endogenous SA, JA, and JA-Ile was performed according to a previous report (Liu et al., 2012).

Callose Staining

Rice seedlings at the four-leaf stage that had been infested by BPH for 24 h were fixed in an ethanol:acetic acid (3:1 v/v) solution for 5 h. The fixative was changed frequently to ensure thorough fixing and clearing of the tissues. The seedlings were then rehydrated successively in 70% ethanol for 2 h, in 50% ethanol for 2 h, and in water overnight. After being washed three times with water, the seedlings were treated with 10% NaOH for 1 h to make the tissues transparent. After rinsing four times with water, the seedlings were incubated in 150 mM K_2HPO_4 (pH 9.5) containing 0.01% aniline blue (Sigma-Aldrich) for 4 h (Millet et al., 2010). The leaf sheaths were mounted on a slide, and callose spots were observed immediately under an Olympus (BX51) microscope under the UV channel.

Subcellular Localization and BiFC Analysis

Protoplasts isolated from etiolated rice seedlings of the Nipponbare cultivar were cotransfected with constructed expressing vectors and subcellular localization marker *DRN-CFP* (Chandler et al., 2011) by previously described procedures. After incubation for 16 to 22 h at 28°C, the protoplasts were imaged under a confocal microscope (Olympus Fluoview FV1000).

Nuclear Fractionation

Rice protoplasts were prepared in extraction buffer 1 (10 mM Tris-HCl at pH 7.5, 10 mM KCl, 0.5% [w/v] Triton X-100, 1.5 mM $MgCl_2$, 340 mM sucrose, and 10% glycerol) and incubated on ice for 10 min. Total soluble proteins were separated by centrifugation at 1000*g* for 20 min in buffer 1 containing 30% Percoll (Sigma-Aldrich). The nuclei-depleted supernatant was separated and the pellet was resuspended in extraction buffer 2 (50 mM Tris-HCl at pH 7.5, 5 mM $MgCl_2$, 1 mM DTT, and 500 mM NaCl), incubated for 10 min, and centrifuged briefly to yield a nuclei-enriched supernatant (Inoue et al., 2013).

Yeast Two-Hybrid Assay

The Matchmaker gold yeast (*Saccharomyces cerevisiae*) two-hybrid system (Clontech) was used to confirm the interactions of the CC, NB, and CN domains or FL BPH14 with itself, and the interaction of the CC, NB, and CN domains or FL BPH14 with WRKY46 or WRKY72. Yeast strain Y2HGold was transformed with the bait plasmid and strain Y187 was transformed with the prey plasmid according to the manufacturer's instructions. Cotransformants were plated on synthetic medium lacking leucine and tryptophan (DDO plates) or synthetic medium lacking leucine, tryptophan, and histidine with 20 μg/mL X-α-Gal and 200 ng/mL Aureobasidin A (AbA) (TDO/X-α-Gal/AbA plates) and incubated at 28 C for 3 d.

WRKY Protection Assay in Protoplasts

Plasmids encoding GFP-Myc or GFP-short-Myc, CC-Myc, NB-Myc, CN-Myc, and FL-Myc were cotransfected with WRKY46-Myc or WRKY72-Myc into protoplasts by the PEG method as described previously (Chen et al., 2006). After incubation for 16 to 22 h, the transfected proteins were detected by protein gel blot analysis.

Yeast One-Hybrid Assay

For protein-DNA interaction studies, the Matchmaker Gold Yeast One-Hybrid Library Screening System (Clontech) was used following the manufacturer's protocol. The GAL4-AD fusion of the murine p53 protein and the bait containing its target sequence (p53DBS) served as controls. The bait constructs were digested with *Bst*BI and transformed into yeast strain Y1HGold, and the transformants were verified by colony PCR. The prey constructs were then transformed into the generated Y1HGold strains that harbored the cognate bait DNA sequences in their genomes. Transformants grown on selective SD medium at 30°C were resuspended in 0.9% NaCl to an OD_{600} of 0.002, or ~2000 cells per 100 μL. Serial dilutions in 0.9% NaCl were dropped onto SD medium supplemented with leucine or 200 ng/mL AbA. Transformants that appeared identical were inspected for the presence of the bait plasmid by colony PCR and for the expression of GAL4-AD-fusion proteins by immunoblot analysis.

EMSA

EMSA was performed as described previously (Kay et al., 2007) with slight modifications. Polyhistidine-tagged fusion proteins of WRKY46 (6×His-WRKY46) and WRKY72 (6×His-WRKY72) were purified from *Escherichia coli* BL21 cells using Ni Sepharose 6 Fast Flow (GE Healthcare; part no.17-5318-01). Protein concentrations were determined by the Bradford assay (Bio-Rad). Complementary pairs of nonlabeled or 5′-biotin-labeled oligonucleotides (Augct) were annealed to obtain double-stranded DNA. DNA primers used for EMSA are listed in Supplemental Data Set 5. EMSA was performed with a LightShift Chemiluminescent EMSA Kit (Thermo Scientific; part no. 20148) and a Chemiluminescent Nucleic Acid Detection Module Kit (Thermo Scientific; part no. 89880) according to the manufacturer's instructions.

Transactivation Assay

The constructs harboring the *CC*, *NB*, and *CN* domains and *FL BPH14*, *WRKY46*, or *WRKY72* were delivered into rice protoplasts by the PEG method together with the appropriate reporter plasmid ($Pro_{RLCK281}$-LUC or

$Pro_{LOC\_Os01g67364.1}$-LUC) as described above. *Pro35S:RLUC* (Renilla luciferase) activity was normalized to the reference LUC activity. Luciferase activity was measured 16 to 22 h after transfection and determined using the Dual-Luciferase Reporter system (Promega) following the manufacturer's instructions.

Reproducibility of Experiments and Statistical Analyses

The presented data generally resulted from a single biological experiment. Unless otherwise stated, equivalent results were obtained in three biologically independent experiments. Statistical analyses were performed by ANOVA (Supplemental Table 1). Mean values were separated by LSD at $P \leq 0.05$.

DNA Isolation and DNA Gel Blot Analysis

Genomic DNA was extracted from the leaves of wild-type Kasalath rice and transgenic plants using the cetyltrimethyl ammonium bromide method. The genomic DNA was digested with the restriction endonucleases *Eco*RI and *Bam*HI, electrophoretically separated on a 1.5% agarose gel, transferred onto a Hybond N^+ membrane (Amersham-Pharmacia), and probed with hygromycin DNA labeled with 5′-biotin (Augct). Pairwise DNA primers hygromycin-F and hygromycin-R are listed in Supplemental Data Set 5. Hybridization and detection of nucleic acid were performed using a North2South Chemiluminescent Hybridization and Detection Kit (Thermo Scientific; part no. 17097) and a Chemiluminescent Nucleic Acid Detection Module Kit (Thermo Scientific; part no. 89880). The membranes were exposed to an appropriately equipped CCD camera (Bio-Rad) to obtain the desired signal.

BPH Survival Rate

To determine the survival rates of nymphs on rice lines, pots (containing one plant each) were individually covered with plastic cages (diameter, 9 cm; height, 12 cm), and 10 third-instar nymphs were released into each cage. The number of surviving BPH nymphs on each plant was recorded every day until 7 d after the introduction of the herbivore. Survival rates were calculated as the number of surviving nymphs divided by the total number of nymphs released at the start of the experiment. Ten experimental replicates were performed for each rice line, with each repeat having 10 BPH insects per rice line in each pot used for analysis.

RNA Isolation and RNA Gel Blot Analysis

Total RNA was extracted from leaf sheaths of 15-d-old seedling tissue (almost at the four-leaf stage) and frozen in liquid nitrogen using TRIzol reagent (Invitrogen), followed by isopropyl alcohol precipitation. The RNA was then dissolved in diethyl pyrocarbonate-treated water. The concentration of RNA was determined by spectrophotometric measurement (Perkin-Elmer). For RNA gel blot analysis, total RNA (40 μg) was separated on a 1.5% formaldehyde agarose denaturing gel and blotted onto Hybond N^+ nylon membranes. Specific sections of *BPH14* cDNA probes were labeled with 5′-biotin. Pairwise DNA primers northernCC-F/northernCC-R and northernNB-F/northernNB-R are listed in Supplemental Data Set 5. Hybridization and nucleic acid detection were performed using a North2South Chemiluminescent Hybridization and Detection Kit (Thermo Scientific; part no. 17097) and a Chemiluminescent Nucleic Acid Detection Module Kit (Thermo Scientific; part no. 89880). The membranes were exposed to an appropriately equipped CCD camera (Bio-Rad) to obtain the desired signal.

Yeast Colony PCR

Single yeast colonies were resuspended in 300 μL lyticase buffer (1.2 M sorbitol, 0.1M sodium phosphate at pH 7.4, and 2.5 mg/mL lyticase [Tiangen; catalog no. RT410]) and incubated for 1 h at 37°C. Yeast plasmid DNA was performed using a TIANprep Yeast Plasmid DNA Kit (Tiangen; catalog no. DP112). Five microliters of the elution was used for PCR with DNA primers pAbAi-F2 and pAbAi-R2 (Supplemental Data Set 5).

Yeast Protein Extraction and Immunoblotting

Yeast protein extraction for immunoblotting analysis was performed using a postalkaline extraction method (Kushnirov, 2000). Single yeast colonies were resuspended in YPDA (1% yeast Extract, 2% peptone, 2% glucose, and 0.003% adenine sulfate) liquid medium to an $OD_{600} = 0.15$ and grown at 30°C and 150 rpm to $OD_{600} = 0.4$ to 0.6. Cells from a 3 mL culture were resuspended in 100 μL distilled water, combined with 100 μL 0.2 M NaOH, incubated for 5 min at room temperature, pelleted, resuspended in 50 μL SDS sample buffer, boiled for 3 min, and pelleted again. Approximately 10 μL protein extract was separated on 10% SDS polyacrylamide gels. Protein fusion detection was performed using anti-HA antibody (MBL; catalog no. M180-3) or anti-Myc antibody (MBL; catalog no. M192-3).

ChIP Experiments

The ChIP experiment was performed following a previously reported protocol (Gendrel et al., 2005) with several modifications. Approximately 9×10^6 cells from each sample of rice protoplasts transfected with WRKY46-Myc or WRKY72-Myc were used as the starting material, and proteins were immunoprecipitated using antibodies against Myc (MBL; catalog no. M192-3). The precipitated DNA was purified with a Qiaquick PCR purification kit (Qiagen; catalog no. 28104) and processed further for ChIP-seq data processing and analysis.

For quantitative analysis of immunoprecipitated chromatin, rice protoplasts were prepared from wild-type Kasalath and transgenic plants with native expression or overexpression of the *CC*, *NB*, and *CN* domains or *FL BPH14*, then transfected with WRKY46-Myc or WRKY72-Myc. Sonicated chromatin fragments were immunoprecipitated with anti-Myc antibody (MBL; catalog no. M192-3). The IP chromatins were analyzed by qPCR using primer pairs CQ1-F/CQ1-R for the promoter region of *RLCK281* and CQ2-F/CQ2-R for the promoter region of LOC_Os01g67364.1 (Supplemental Data Set 6). The non-IP and sonicated chromatin was used as the total input DNA control. The percentage of immunoprecipitation (IP%) was used to compare different samples by calculating the ratio of the amount of target PCR product from IP relative to that from the input. The IP% was calculated using the following formula: $IP\% = 2^{-\Delta Ct\ (normalized\ ChIP)}$, in which ΔCycle threshold (ΔCt) = Ct [ChIP] − (Ct [input] − $\log_2$ input dilution factor) and input dilution factor = (fraction of the input chromatin saved)$^{-1}$ in the qPCR, according to a previous report (Haring et al., 2007).

Accession Numbers

Sequence data from this article can be found in the GenBank Database or Rice Genome Annotation Project under the following accession numbers: *BPH14* (FJ941067.1), *WRKY46* (BK005049), *WRKY47* (BK005050), *WRKY51* (BK005053), *WRKY62* (BK005065), *WRKY67* (BK005070), *WRKY68* (BK005071), *WRKY69* (BK005072), *WRKY72* (BK005075), *WRKY74* (BK005077), *RLCK281* (LOC_Os09g39640.1), LOC_Os01g67364.1 (LOC_Os01g67364.1), *EDS1* (AK100117), *PAL* (X87946), *ICS1* (AK120689), *NPR1* (AY923983), *LOX* (D14000), *AOS2* (AY062258), *PR1b* (U89895), *PR4* (AY050642), *PR5* (X68179), *PR10* (D38170), *GNS5* (U72251), *GNS6* (U72252), *GNS8* (U72254), *GNS9* (U72255), and *OsACTIN1* (AB047313). The ChIP-seq data created in this study have been deposited in the Gene Expression Omnibus repository (GSE93607).

Supplemental Data

Supplemental Figure 1. DNA gel blot analysis of homozygous transgenic plants.

Supplemental Figure 2. Protein expression of BPH14 and the derived fragments in transgenic and wild-type plants.

Supplemental Figure 3. BPH survival rate on *BPH14*- and *CC*, *NB*, and *CN* domain-expressing transgenic plants.

Supplemental Figure 4. Expression of the *CC* domain, *NB* domain, *CN* domain, and *FL BPH14* in wild-type and transgenic plants.

Supplemental Figure 5. BPH resistance test of *BPH14*- and *CC*, *NB*, and *CN* domain-expressing transgenic and wild-type rice.

Supplemental Figure 6. Characterization of insect resistance in *BPH14*- and *CC*, *NB*, and *CN* domain-expressing transgenic rice.

Supplemental Figure 7. Phenotypes of *CC*, *NB*, and *CN* domain and *BPH14* transgenic plants.

Supplemental Figure 8. ROS generation in *CC*, *NB*, and *CN* domain- or *FL BPH14*-overexpressing rice protoplast lines.

Supplemental Figure 9. Expression analysis of plant callose-related genes in *BPH14*- and *CC*, *NB*, and *CN* domain-expressing transgenic and wild-type rice.

Supplemental Figure 10. Accumulation of bait and prey proteins in yeast.

Supplemental Figure 11. Screening of several rice WRKY proteins with BPH14 identified two different BPH14 interactor clones (WRKY46 and WRKY72).

Supplemental Figure 12. Verification of negative control proteins tested in the BiFC experiments.

Supplemental Figure 13. Expression analysis of *WRKY46* and *WRKY72* in *BPH14*- and *CC*, *NB*, and *CN* domain-expressing transgenic and wild-type rice.

Supplemental Figure 14. Putative promoter sequences and DNA probes of *RLCK281* and LOC_Os01g67364.1.

Supplemental Figure 15. Verification of DNA bait and prey proteins in yeast.

Supplemental Figure 16. Competitive binding assays of W-box$_{RLCK281}$ and W-box$_{LOC_Os01g67364.1}$ probe to 6×His-WRKY46 and 6×His-WRKY72.

Supplemental Table 1. ANOVA tables.

Supplemental Data Set 1. Traits of wild-type Kasalath and *CC*, *NB*, and *CN* domain- and *BPH14*-expressing transgenic plants.

Supplemental Data Set 2. List of genes significantly enriched ($P < 0.05$) in rice protoplasts transfected with WRKY46-Myc in a ChIP assay.

Supplemental Data Set 3. List of genes significantly enriched ($P < 0.05$) in rice protoplasts transfected with WRKY72-Myc in a ChIP assay.

Supplemental Data Set 4. Details of the gene constructs used in this study.

Supplemental Data Set 5. List of PCR primers used in this study.

Supplemental Data Set 6. List of qPCR primers used in this study.

ACKNOWLEDGMENTS

This work was supported by grants from National Key Research and Development Program (2016YFD0100600), the National Program on Research & Development of Transgenic Plants (2016ZX08009-003-001), and the National Natural Science Foundation of China (31630063).

AUTHOR CONTRIBUTIONS

G.C.H. and L.H. designed research. L.H., Y.W., D.W., W.W.R., J.P.G., Y.H.M., Z.Z.W., X.X.S.G., H.Y.W., C.X.X., J.H., and S.J.S. participated in the experiments. G.C.H., L.H., R.Z.C., and B.D. analyzed the data. L.L.Z. prepared the experimental reagents. G.C.H. and L.H wrote the article.

Received April 4, 2017; revised October 4, 2017; accepted October 31, 2017; published November 1, 2017.

REFERENCES

Abbruscato, P., et al. (2012). *OsWRKY22*, a monocot WRKY gene, plays a role in the resistance response to blast. Mol. Plant Pathol. **13:** 828–841.

Ade, J., DeYoung, B.J., Golstein, C., and Innes, R.W. (2007). Indirect activation of a plant nucleotide binding site-leucine-rich repeat protein by a bacterial protease. Proc. Natl. Acad. Sci. USA **104:** 2531–2536.

Bacsó, R., Hafez, Y., Király, Z., and Király, L. (2011). Inhibition of virus replication and symptom expression by reactive oxygen species in tobacco infected with *Tobacco mosaic virus.* Acta Phytopathol. Entomol. Hung. **46:** 1–10.

Bai, S., Liu, J., Chang, C., Zhang, L., Maekawa, T., Wang, Q., Xiao, W., Liu, Y., Chai, J., Takken, F.L., Schulze-Lefert, P., and Shen, Q.H. (2012). Structure-function analysis of barley NLR immune receptor MLA10 reveals its cell compartment specific activity in cell death and disease resistance. PLoS Pathog. **8:** e1002752.

Bendahmane, A., Farnham, G., Moffett, P., and Baulcombe, D.C. (2002). Constitutive gain-of-function mutants in a nucleotide binding site-leucine rich repeat protein encoded at the *Rx* locus of potato. Plant J. **32:** 195–204.

Bendahmane, A., Kanyuka, K., and Baulcombe, D.C. (1999). The *Rx* gene from potato controls separate virus resistance and cell death responses. Plant Cell **11:** 781–792.

Bhattacharjee, S., Zamora, A., Azhar, M.T., Sacco, M.A., Lambert, L.H., and Moffett, P. (2009). Virus resistance induced by NB-LRR proteins involves Argonaute4-dependent translational control. Plant J. **58:** 940–951.

Blümke, A., Falter, C., Herrfurth, C., Sode, B., Bode, R., Schäfer, W., Feussner, I., and Voigt, C.A. (2014). Secreted fungal effector lipase releases free fatty acids to inhibit innate immunity-related callose formation during wheat head infection. Plant Physiol. **165:** 346–358.

Blümke, A., Somerville, S.C., and Voigt, C.A. (2013). Transient expression of the *Arabidopsis thaliana* callose synthase PMR4 increases penetration resistance to powdery mildew in barley. Adv. Biosci. Biotechnol. **4:** 810–813.

Boller, T., and Felix, G. (2009). A renaissance of elicitors: perception of microbe-associated molecular patterns and danger signals by pattern-recognition receptors. Annu. Rev. Plant Biol. **60:** 379–406.

Boyes, D.C., Nam, J., and Dangl, J.L. (1998). The *Arabidopsis thaliana RPM1* disease resistance gene product is a peripheral plasma membrane protein that is degraded coincident with the hypersensitive response. Proc. Natl. Acad. Sci. USA **95:** 15849–15854.

Browse, J. (2009). Jasmonate passes muster: a receptor and targets for the defense hormone. Annu. Rev. Plant Biol. **60:** 183–205.

Brunner, S., Hurni, S., Herren, G., Kalinina, O., von Burg, S., Zeller, S.L., Schmid, B., Winzeler, M., and Keller, B. (2011). Transgenic *Pm3b* wheat lines show resistance to powdery mildew in the field. Plant Biotechnol. J. **9:** 897–910.

Bulgarelli, D., Biselli, C., Collins, N.C., Consonni, G., Stanca, A.M., Schulze-Lefert, P., and Valè, G. (2010). The CC-NB-LRR-type *Rdg2a* resistance gene confers immunity to the seed-borne barley leaf stripe pathogen in the absence of hypersensitive cell death. PLoS One **5:** e12599.

Casey, L.W., et al. (2016). The CC domain structure from the wheat stem rust resistance protein Sr33 challenges paradigms for dimerization in plant NLR proteins. Proc. Natl. Acad. Sci. USA **113:** 12856–12861.

Casteel, C.L., Walling, L.L., and Paine, T.D. (2006). Behavior and biology of the tomato psyllid, *Bactericerca cockerelli*, in response to the *Mi-1.2* gene. Entomol. Exp. Appl. **121:** 67–72.

Cesari, S., Moore, J., Chen, C., Webb, D., Periyannan, S., Mago, R., Bernoux, M., Lagudah, E.S., and Dodds, P.N. (2016). Cytosolic activation of cell death and stem rust resistance by cereal MLA-family CC-NLR proteins. Proc. Natl. Acad. Sci. USA **113:** 10204–10209.

Chandler, J.W., Cole, M., Jacobs, B., Comelli, P., and Werr, W. (2011). Genetic integration of DORNRÖSCHEN and DORNRÖSCHEN-LIKE reveals hierarchical interactions in auxin signalling and patterning of the *Arabidopsis* apical embryo. Plant Mol. Biol. **75:** 223–236.

Chang, C., Yu, D., Jiao, J., Jing, S., Schulze-Lefert, P., and Shen, Q.H. (2013). Barley MLA immune receptors directly interfere with antagonistically acting transcription factors to initiate disease resistance signaling. Plant Cell **25:** 1158–1173.

Chen, H., Wang, S., Xing, Y., Xu, C., Hayes, P.M., and Zhang, Q. (2003). Comparative analyses of genomic locations and race specificities of loci for quantitative resistance to *Pyricularia grisea* in rice and barley. Proc. Natl. Acad. Sci. USA **100:** 2544–2549.

Chen, H., Wang, S., and Zhang, Q. (2002). New gene for bacterial blight resistance in rice located on chromosome 12 identified from minghui 63, an elite restorer line. Phytopathology **92:** 750–754.

Chen, S., Songkumarn, P., Liu, J., and Wang, G.L. (2009). A versatile zero background T-vector system for gene cloning and functional genomics. Plant Physiol. **150:** 1111–1121.

Chen, S., Tao, L., Zeng, L., Vega-Sanchez, M.E., Umemura, K., and Wang, G.L. (2006). A highly efficient transient protoplast system for analyzing defence gene expression and protein-protein interactions in rice. Mol. Plant Pathol. **7:** 417–427.

Chi, Y., Yang, Y., Zhou, Y., Zhou, J., Fan, B., Yu, J.Q., and Chen, Z. (2013). Protein-protein interactions in the regulation of WRKY transcription factors. Mol. Plant **6:** 287–300.

Coll, N.S., Epple, P., and Dangl, J.L. (2011). Programmed cell death in the plant immune system. Cell Death Differ. **18:** 1247–1256.

Collier, S.M., and Moffett, P. (2009). NB-LRRs work a "bait and switch" on pathogens. Trends Plant Sci. **14:** 521–529.

Collier, S.M., Hamel, L.P., and Moffett, P. (2011). Cell death mediated by the N-terminal domains of a unique and highly conserved class of NB-LRR protein. Mol. Plant Microbe Interact. **24:** 918–931.

Dai, X., Wang, Y., and Zhang, W.H. (2016). *OsWRKY74*, a WRKY transcription factor, modulates tolerance to phosphate starvation in rice. J. Exp. Bot. **67:** 947–960.

Dangl, J.L., Horvath, D.M., and Staskawicz, B.J. (2013). Pivoting the plant immune system from dissection to deployment. Science **341:** 746–751.

Danot, O., Marquenet, E., Vidal-Ingigliardi, D., and Richet, E. (2009). Wheel of life, wheel of death: a mechanistic insight into signaling by STAND proteins. Structure **17:** 172–182.

De Oliveira, A.S., Koolhaas, I., Boiteux, L.S., Caldararu, O.F., Petrescu, A.J., Oliveira Resende, R., and Kormelink, R. (2016). Cell death triggering and effector recognition by Sw-5 SD-CNL proteins from resistant and susceptible tomato isolines to Tomato spotted wilt virus. Mol. Plant Pathol. **17:** 1442–1454.

Dogimont, C., Chovelon, V., Pauquet, J., Boualem, A., and Bendahmane, A. (2014). The Vat locus encodes for a CC-NBS-LRR protein that confers resistance to *Aphis gossypii* infestation and *A. gossypii*-mediated virus resistance. Plant J. **80:** 993–1004.

Dong, J., Chen, C., and Chen, Z. (2003). Expression profiles of the *Arabidopsis* WRKY gene superfamily during plant defense response. Plant Mol. Biol. **51:** 21–37.

Dong, X., Hong, Z., Chatterjee, J., Kim, S., and Verma, D.P.S. (2008). Expression of callose synthase genes and its connection with *Npr1* signaling pathway during pathogen infection. Planta **229:** 87–98.

Du, B., Zhang, W., Liu, B., Hu, J., Wei, Z., Shi, Z., He, R., Zhu, L., Chen, R., Han, B., and He, G. (2009). Identification and characterization of *Bph14*, a gene conferring resistance to brown planthopper in rice. Proc. Natl. Acad. Sci. USA **106:** 22163–22168.

Dubouzet, J.G., et al. (2011). Screening for resistance against *Pseudomonas syringae* in rice-FOX *Arabidopsis* lines identified a putative receptor-like cytoplasmic kinase gene that confers resistance to major bacterial and fungal pathogens in *Arabidopsis* and rice. Plant Biotechnol. J. **9:** 466–485.

Ellinger, D., Naumann, M., Falter, C., Zwikowics, C., Jamrow, T., Manisseri, C., Somerville, S.C., and Voigt, C.A. (2013). Elevated early callose deposition results in complete penetration resistance to powdery mildew in *Arabidopsis.* Plant Physiol. **161:** 1433–1444.

Enrique, R., Siciliano, F., Favaro, M.A., Gerhardt, N., Roeschlin, R., Rigano, L., Sendin, L., Castagnaro, A., Vojnov, A., and Marano, M.R. (2011). Novel demonstration of RNAi in citrus reveals importance of citrus callose synthase in defence against *Xanthomonas citri* subsp. *citri.* Plant Biotechnol. J. **9:** 394–407.

Feng, F., Yang, F., Rong, W., Wu, X., Zhang, J., Chen, S., He, C., and Zhou, J.M. (2012). A *Xanthomonas* uridine 5′-monophosphate transferase inhibits plant immune kinases. Nature **485:** 114–118.

Fenyk, S., Campillo, Ade.S., Pohl, E., Hussey, P.J., and Cann, M.J. (2012). A nucleotide phosphatase activity in the nucleotide binding domain of an orphan resistance protein from rice. J. Biol. Chem. **287:** 4023–4032.

Fenyk, S., Dixon, C.H., Gittens, W.H., Townsend, P.D., Sharples, G.J., Pålsson, L.O., Takken, F.L., and Cann, M.J. (2016). The tomato nucleotide-binding leucine-rich repeat Immune receptor I-2 couples DNA-binding to nucleotide-binding domain nucleotide exchange. J. Biol. Chem. **291:** 1137–1147.

Fenyk, S., et al. (2015). The potato nucleotide-binding leucine-rich repeat (NLR) immune receptor Rx1 is a pathogen-dependent DNA-deforming protein. J. Biol. Chem. **290:** 24945–24960.

Foyer, C.H., and Noctor, G. (2005). Redox homeostasis and antioxidant signaling: a metabolic interface between stress perception and physiological responses. Plant Cell **17:** 1866–1875.

Freialdenhoven, A., Scherag, B., Hollricher, K., Collinge, D.B., Thordal-Christensen, H., and Schulze-Lefert, P. (1994). Nar-1 and Nar-2, two loci required for Mla12-specified race-specific resistance to powdery mildew in barley. Plant Cell **6:** 983–994.

Gao, Z., Chung, E.H., Eitas, T.K., and Dangl, J.L. (2011). Plant intracellular innate immune receptor Resistance to *Pseudomonas syringae pv. maculicola 1* (RPM1) is activated at, and functions on, the plasma membrane. Proc. Natl. Acad. Sci. USA **108:** 7619–7624. Erratum. Proc. Natl. Acad. Sci. USA **108:** 8915.

Gassmann, W. (2005). Natural variation in the *Arabidopsis* response to the avirulence gene *hopPsyA* uncouples the hypersensitive response from disease resistance. Mol. Plant Microbe Interact. **18:** 1054–1060.

Ge, X.M., Cai, H.L., Lei, X., Zhou, X., Yue, M., and He, J.M. (2015). Heterotrimeric G protein mediates ethylene-induced stomatal closure via hydrogen peroxide synthesis in *Arabidopsis.* Plant J. **82:** 138–150.

Gendrel, A.V., Lippman, Z., Martienssen, R., and Colot, V. (2005). Profiling histone modification patterns in plants using genomic tiling microarrays. Nat. Methods **2:** 213–218.

Grist, D.H., and Lever, R.J.A.W. (1969). Pests of Rice. (London: Longmans, Green and Company).

Gutierrez, J.R., Balmuth, A.L., Ntoukakis, V., Mucyn, T.S., Gimenez-Ibanez, S., Jones, A.M., and Rathjen, J.P. (2010). Prf immune complexes of tomato are oligomeric and contain multiple Pto-like kinases that diversify effector recognition. Plant J. **61:** 507–518.

Hafez, Y.M., and Kiraly, Z. (2003). Role of hydrogen peroxide in symptom expression of barley susceptible and resistant to powdery mildew. Acta Phytopathol. Entomol. Hung. **38:** 227–236.

Hao, P., Liu, C., Wang, Y., Chen, R., Tang, M., Du, B., Zhu, L., and He, G. (2008). Herbivore-induced callose deposition on the sieve plates of rice: an important mechanism for host resistance. Plant Physiol. **146:** 1810–1820.

Haring, M., Offermann, S., Danker, T., Horst, I., Peterhansel, C., and Stam, M. (2007). Chromatin immunoprecipitation: optimization, quantitative analysis and data normalization. Plant Methods **3:** 11.

Heidrich, K., Wirthmueller, L., Tasset, C., Pouzet, C., Deslandes, L., and Parker, J.E. (2011). *Arabidopsis* EDS1 connects pathogen effector recognition to cell compartment-specific immune responses. Science **334:** 1401–1404.

Henry, E., Fung, N., Liu, J., Drakakaki, G., and Coaker, G. (2015). Beyond glycolysis: GAPDHs are multi-functional enzymes involved in regulation of ROS, autophagy, and plant immune responses. PLoS Genet. **11:** e1005199.

Ho, S.N., Hunt, H.D., Horton, R.M., Pullen, J.K., and Pease, L.R. (1989). Site-directed mutagenesis by overlap extension using the polymerase chain reaction. Gene **77:** 51–59.

Horton, R.M., Hunt, H.D., Ho, S.N., Pullen, J.K., and Pease, L.R. (1989). Engineering hybrid genes without the use of restriction enzymes: gene splicing by overlap extension. Gene **77:** 61–68.

Hou, Y., Qiu, J., Tong, X., Wei, X., Nallamilli, B.R., Wu, W., Huang, S., and Zhang, J. (2015). A comprehensive quantitative phosphoproteome analysis of rice in response to bacterial blight. BMC Plant Biol. **15:** 163.

Howles, P., Lawrence, G., Finnegan, J., McFadden, H., Ayliffe, M., Dodds, P., and Ellis, J. (2005). Autoactive alleles of the flax *L6* rust resistance gene induce non-race-specific rust resistance associated with the hypersensitive response. Mol. Plant Microbe Interact. **18:** 570–582.

Hu, J., Zhou, J., Peng, X., Xu, H., Liu, C., Du, B., Yuan, H., Zhu, L., and He, G. (2011). The *Bphi008a* gene interacts with the ethylene pathway and transcriptionally regulates MAPK genes in the response of rice to brown planthopper feeding. Plant Physiol. **156:** 856–872.

Hu, Z., Zhou, Q., Zhang, C., Fan, S., Cheng, W., Zhao, Y., Shao, F., Wang, H.W., Sui, S.F., and Chai, J. (2015). Structural and biochemical basis for induced self-propagation of NLRC4. Science **350:** 399–404.

Huang, Z., He, G.C., Shu, L.H., Li, X.H., and Zhang, Q.F. (2001). Identification and mapping of two brown planthopper resistance genes in rice. Theor. Appl. Genet. **102:** 929–934.

Inoue, H., Hayashi, N., Matsushita, A., Xinqiong, L., Nakayama, A., Sugano, S., Jiang, C.J., and Takatsuji, H. (2013). Blast resistance of CC-NB-LRR protein Pb1 is mediated by WRKY45 through protein-protein interaction. Proc. Natl. Acad. Sci. USA **110:** 9577–9582.

International Rice Research Institute (2002). Standard Evaluation System for Rice. (Los Banos, Philippines: International Rice Research Institute).

Jacob, F., Vernaldi, S., and Maekawa, T. (2013). Evolution and conservation of plant NLR functions. Front. Immunol. **4:** 297–312.

Jacobs, A.K., Lipka, V., Burton, R.A., Panstruga, R., Strizhov, N., Schulze-Lefert, P., and Fincher, G.B. (2003). An *Arabidopsis* callose synthase, GSL5, is required for wound and papillary callose formation. Plant Cell **15:** 2503–2513.

Ji, H., and Kim, et al. (2016). Map-based cloning and characterization of the *BPH18* gene from wild rice conferring resistance to brown planthopper (BPH) insect pest. Sci. Rep. **6:** 34376.

Jones, J.D., and Dangl, J.L. (2006). The plant immune system. Nature **444:** 323–329.

Künstler, A., Bacsó, R., Gullner, G., Hafez, Y.M., and Király, L. (2016). Staying alive - is cell death dispensable for plant disease resistance during the hypersensitive response? Physiol. Mol. Plant Pathol. **93:** 75–84.

Kay, S., Hahn, S., Marois, E., Hause, G., and Bonas, U. (2007). A bacterial effector acts as a plant transcription factor and induces a cell size regulator. Science **318:** 648–651.

Khare, E., Kim, K., and Lee, K.J. (2016). Rice *OsPBL1* (ORYZA SATIVA *ARABIDOPSIS* PBS1-LIKE 1) enhanced defense of *Arabidopsis* against *Pseudomonas syringae* DC3000. Eur. J. Plant Pathol. **146:** 901–910.

Kombrink, E., and Schmelzer, E. (2001). The hypersensitive response and its role in local and systemic disease resistance. Eur. J. Plant Pathol. **107:** 69–78.

Kong, Q., Sun, T., Qu, N., Ma, J., Li, M., Cheng, Y.T., Zhang, Q., Wu, D., Zhang, Z., and Zhang, Y. (2016). Two redundant receptor-like cytoplasmic kinases function downstream of pattern recognition receptors to regulate activation of SA biosynthesis. Plant Physiol. **171:** 1344–1354.

Kushnirov, V.V. (2000). Rapid and reliable protein extraction from yeast. Yeast **16:** 857–860.

Laemmli, U.K. (1970). Cleavage of structural proteins during the assembly of the head of bacteriophage T4. Nature **227:** 680–685.

Lehnackers, H., and Knogge, W. (1990). Cytological studies on the infection of barley cultivars with known resistance genotypes by *Rhynchosporiumsecalis.* Can. J. Bot. **68:** 1953–1961.

Leipe, D.D., Koonin, E.V., and Aravind, L. (2004). STAND, a class of P-loop NTPases including animal and plant regulators of programmed cell death: multiple, complex domain architectures, unusual phyletic patterns, and evolution by horizontal gene transfer. J. Mol. Biol. **343:** 1–28.

Lewis, J.D., Lee, A.H.Y., Hassan, J.A., Wan, J., Hurley, B., Jhingree, J.R., Wang, P.W., Lo, T., Youn, J.Y., Guttman, D.S., and Desveaux, D. (2013). The *Arabidopsis* ZED1 pseudokinase is required for ZAR1-mediated immunity induced by the *Pseudomonas syringae* type III effector HopZ1a. Proc. Natl. Acad. Sci. USA **110:** 18722–18727.

Li, Q., Xie, Q.G., Smith-Becker, J., Navarre, D.A., and Kaloshian, I. (2006). *Mi-1*-Mediated aphid resistance involves salicylic acid and mitogen-activated protein kinase signaling cascades. Mol. Plant Microbe Interact. **19:** 655–664.

Liu, H., Li, X., Xiao, J., and Wang, S. (2012). A convenient method for simultaneous quantification of multiple phytohormones and metabolites: application in study of rice-bacterium interaction. Plant Methods **8:** 2.

Liu, J., Elmore, J.M., Lin, Z.J.D., and Coaker, G. (2011). A receptor-like cytoplasmic kinase phosphorylates the host target RIN4, leading to the activation of a plant innate immune receptor. Cell Host Microbe **9:** 137–146.

Livak, K.J., and Schmittgen, T.D. (2001). Analysis of relative gene expression data using real-time quantitative PCR and the 2(-Delta Delta C(T)) method. Methods **25:** 402–408.

Lu, A., Li, Y., Schmidt, F.I., Yin, Q., Chen, S., Fu, T.M., Tong, A.B., Ploegh, H.L., Mao, Y., and Wu, H. (2016). Molecular basis of

caspase-1 polymerization and its inhibition by a new capping mechanism. Nat. Struct. Mol. Biol. **23:** 416–425.

Maekawa, T., et al. (2011). Coiled-coil domain-dependent homodimerization of intracellular barley immune receptors defines a minimal functional module for triggering cell death. Cell Host Microbe **9:** 187–199.

Martin, G.B., Frary, A., Wu, T., Brommonschenkel, S., Chunwongse, J., Earle, E.D., and Tanksley, S.D. (1994). A member of the tomato Pto gene family confers sensitivity to fenthion resulting in rapid cell death. Plant Cell **6:** 1543–1552.

Martinez de Ilarduya, O., Xie, Q., and Kaloshian, I. (2003). Aphid-induced defense responses in Mi-1-mediated compatible and incompatible tomato interactions. Mol. Plant Microbe Interact. **16:** 699–708.

Matsushita, A., Inoue, H., Goto, S., Nakayama, A., Sugano, S., Hayashi, N., and Takatsuji, H. (2013). Nuclear ubiquitin proteasome degradation affects WRKY45 function in the rice defense program. Plant J. **73:** 302–313.

Millet, Y.A., Danna, C.H., Clay, N.K., Songnuan, W., Simon, M.D., Werck-Reichhart, D., and Ausubel, F.M. (2010). Innate immune responses activated in *Arabidopsis* roots by microbe-associated molecular patterns. Plant Cell **22:** 973–990.

Mittler, R., Vanderauwera, S., Suzuki, N., Miller, G., Tognetti, V.B., Vandepoele, K., Gollery, M., Shulaev, V., and Van Breusegem, F. (2011). ROS signaling: the new wave? Trends Plant Sci. **16:** 300–309.

Nishimura, A., Ashikari, M., Lin, S., Takashi, T., Angeles, E.R., Yamamoto, T., and Matsuoka, M. (2005). Isolation of a rice regeneration quantitative trait loci gene and its application to transformation systems. Proc. Natl. Acad. Sci. USA **102:** 11940–11944.

Nishinaka, Y., Aramaki, Y., Yoshida, H., Masuya, H., Sugawara, T., and Ichimori, Y. (1993). A new sensitive chemiluminescence probe, L-012, for measuring the production of superoxide anion by cells. Biochem. Biophys. Res. Commun. **193:** 554–559.

Nombela, G., Williamson, V.M., and Muñiz, M. (2003). The root-knot nematode resistance gene *Mi-1.2* of tomato is responsible for resistance against the whitefly *Bemisia tabaci*. Mol. Plant Microbe Interact. **16:** 645–649.

Ntoukakis, V., Saur, I.M., Conlan, B., and Rathjen, J.P. (2014). The changing of the guard: the Pto/Prf receptor complex of tomato and pathogen recognition. Curr. Opin. Plant Biol. **20:** 69–74.

Oldroyd, G.E.D., and Staskawicz, B.J. (1998). Genetically engineered broad-spectrum disease resistance in tomato. Proc. Natl. Acad. Sci. USA **95:** 10300–10305.

Pérez, F., and Rubio, S. (2006). An improved chemiluminescence method for hydrogen peroxide determination in plant tissues. J. Plant Growth Regul. **48:** 89–95.

Padmanabhan, M.S., Ma, S., Burch-Smith, T.M., Czymmek, K., Huijser, P., and Dinesh-Kumar, S.P. (2013). Novel positive regulatory role for the SPL6 transcription factor in the N TIR-NB-LRR receptor-mediated plant innate immunity. PLoS Pathog. **9:** e1003235.

Painter, R.H. (1951). Insect Resistance in Crop Plants. (New York: The Macmillan Company).

Park, C.J., and Ronald, P.C. (2012). Cleavage and nuclear localization of the rice XA21 immune receptor. Nat. Commun. **3:** 920.

Pathak, P.K., Saxena, R.C., and Heinrichs, E.A. (1982). Parafilm sachet for measuring honeydew excretion by *Nilaparvata lugens* on rice. J. Econ. Entomol. **75:** 194–195.

Peng, Y., Bartley, L.E., Chen, X., Dardick, C., Chern, M., Ruan, R., Canlas, P.E., and Ronald, P.C. (2008). OsWRKY62 is a negative regulator of basal and *Xa21*-mediated defense against *Xanthomonas oryzae* pv. *oryzae* in rice. Mol. Plant **1:** 446–458.

Proell, M., Riedl, S.J., Fritz, J.H., Rojas, A.M., and Schwarzenbacher, R. (2008). The Nod-like receptor (NLR) family: a tale of similarities and differences. PLoS One **3:** e2119.

Qi, S., et al. (2010). Crystal structure of the *Caenorhabditis elegans* apoptosome reveals an octameric assembly of CED-4. Cell **141:** 446–457.

Qiu, Y., Guo, J., Jing, S., Tang, M., Zhu, L., and He, G. (2011). Identification of antibiosis and tolerance in rice varieties carrying brown planthopper resistance genes. Entomol. Exp. Appl. **141:** 224–231.

Rairdan, G.J., Collier, S.M., Sacco, M.A., Baldwin, T.T., Boettrich, T., and Moffett, P. (2008). The coiled-coil and nucleotide binding domains of the Potato Rx disease resistance protein function in pathogen recognition and signaling. Plant Cell **20:** 739–751.

Sato, Y., Ando, S., and Takahashi, H. (2014). Role of intron-mediated enhancement on accumulation of an *Arabidopsis* NB-LRR class R-protein that confers resistance to *Cucumber mosaic virus.* PLoS One **9:** e99041.

Schultz, J.C. (2002). Biochemical ecology: how plants fight dirty. Nature **416:** 267.

Sels, J., Mathys, J., De Coninck, B.M., Cammue, B.P., and De Bolle, M.F. (2008). Plant pathogenesis-related (PR) proteins: a focus on PR peptides. Plant Physiol. Biochem. **46:** 941–950.

Shen, Q.H., Saijo, Y., Mauch, S., Biskup, C., Bieri, S., Keller, B., Seki, H., Ulker, B., Somssich, I.E., and Schulze-Lefert, P. (2007). Nuclear activity of MLA immune receptors links isolate-specific and basal disease-resistance responses. Science **315:** 1098–1103.

Shi, H., Yan, H., Li, J., and Tang, D. (2013). BSK1, a receptor-like cytoplasmic kinase, involved in both BR signaling and innate immunity in *Arabidopsis.* Plant Signal. Behav. **8:** e24996.

Shinya, T., et al. (2014). Selective regulation of the chitin-induced defense response by the *Arabidopsis* receptor-like cytoplasmic kinase PBL27. Plant J. **79:** 56–66.

Slootweg, E., et al. (2010). Nucleocytoplasmic distribution is required for activation of resistance by the potato NB-LRR receptor Rx1 and is balanced by its functional domains. Plant Cell **22:** 4195–4215.

Slootweg, E.J., Spiridon, L.N., Roosien, J., Butterbach, P., Pomp, R., Westerhof, L., Wilbers, R., Bakker, E., Bakker, J., Petrescu, A.J., Smant, G., and Goverse, A. (2013). Structural determinants at the interface of the ARC2 and leucine-rich repeat domains control the activation of the plant immune receptors Rx1 and Gpa2. Plant Physiol. **162:** 1510–1528.

Smith, C.M., and Clement, S.L. (2012). Molecular bases of plant resistance to arthropods. Annu. Rev. Entomol. **57:** 309–328.

Stirnweis, D., Milani, S.D., Brunner, S., Herren, G., Buchmann, G., Peditto, D., Jordan, T., and Keller, B. (2014). Suppression among alleles encoding nucleotide-binding-leucine-rich repeat resistance proteins interferes with resistance in F1 hybrid and allele-pyramided wheat plants. Plant J. **79:** 893–903.

Swiderski, M.R., and Innes, R.W. (2001). The *Arabidopsis PBS1* resistance gene encodes a member of a novel protein kinase subfamily. Plant J. **26:** 101–112.

Takken, F.L., and Goverse, A. (2012). How to build a pathogen detector: structural basis of NB-LRR function. Curr. Opin. Plant Biol. **15:** 375–384.

Tameling, W.I.L., Elzinga, S.D.J., Darmin, P.S., Vossen, J.H., Takken, F.L.W., Haring, M.A., and Cornelissen, B.J.C. (2002). The tomato *R* gene products I-2 and MI-1 are functional ATP binding proteins with ATPase activity. Plant Cell **14:** 2929–2939.

Tameling, W.I.L., Vossen, J.H., Albrecht, M., Lengauer, T., Berden, J.A., Haring, M.A., Cornelissen, B.J., and Takken, F.L. (2006). Mutations in the NB-ARC domain of I-2 that impair ATP hydrolysis cause autoactivation. Plant Physiol. **140:** 1233–1245.

Tamura, Y., Hattori, M., Yoshioka, H., Yoshioka, M., Takahashi, A., Wu, J., Sentoku, N., and Yasui, H. (2014). Map-based cloning and characterization of a brown planthopper resistance gene *BPH26* from *Oryza sativa L. ssp. indica* cultivar ADR52. Sci. Rep. **4:** 5872.

Tao, Y., Xie, Z., Chen, W., Glazebrook, J., Chang, H.S., Han, B., Zhu, T., Zou, G., and Katagiri, F. (2003). Quantitative nature of Arabidopsis responses during compatible and incompatible interactions with the bacterial pathogen *Pseudomonas syringae.* Plant Cell **15:** 317–330.

Tao, Y., Yuan, F., Leister, R.T., Ausubel, F.M., and Katagiri, F. (2000). Mutational analysis of the *Arabidopsis* nucleotide binding site-leucine-rich repeat resistance gene *RPS2.* Plant Cell **12:** 2541–2554.

Ueda, H., Yamaguchi, Y., and Sano, H. (2006). Direct interaction between the tobacco mosaic virus helicase domain and the ATP-bound resistance protein, N factor during the hypersensitive response in tobacco plants. Plant Mol. Biol. **61:** 31–45.

Vanaja, S.K., Rathinam, V.A.K., and Fitzgerald, K.A. (2015). Mechanisms of inflammasome activation: recent advances and novel insights. Trends Cell Biol. **25:** 308–315.

van Ooijen, G., Mayr, G., Albrecht, M., Cornelissen, B.J., and Takken, F.L. (2008). Transcomplementation, but not physical association of the CC-NB-ARC and LRR domains of tomato R protein Mi-1.2 is altered by mutations in the ARC2 subdomain. Mol. Plant **1:** 401–410.

Vij, S., Giri, J., Dansana, P.K., Kapoor, S., and Tyagi, A.K. (2008). The receptor-like cytoplasmic kinase (*OsRLCK*) gene family in rice: organization, phylogenetic relationship, and expression during development and stress. Mol. Plant **1:** 732–750.

von Moltke, J., Ayres, J.S., Kofoed, E.M., Chavarría-Smith, J., and Vance, R.E. (2013). Recognition of bacteria by inflammasomes. Annu. Rev. Immunol. **31:** 73–106.

Vos, P., et al. (1998). The tomato *Mi-1* gene confers resistance to both root-knot nematodes and potato aphids. Nat. Biotechnol. **16:** 1365–1369.

Walling, L.L. (2000). The myriad plant responses to herbivores. J. Plant Growth Regul. **19:** 195–216.

Walter, M., Chaban, C., Schütze, K., Batistic, O., Weckermann, K., Näke, C., Blazevic, D., Grefen, C., Schumacher, K., Oecking, C., Harter, K., and Kudla, J. (2004). Visualization of protein interactions in living plant cells using bimolecular fluorescence complementation. Plant J. **40:** 428–438.

Wang, G.F., Ji, J., Ei-Kasmi, F., Dangl, J.L., Johal, G., and Balint-Kurti, P.J. (2015a). Correction: Molecular and functional analyses of a maize autoactive NB-LRR protein identify precise structural requirements for activity. PLoS Pathog. **11:** e1004830.

Wang, J., et al. (2015b). The receptor-like cytoplasmic kinase OsRLCK102 regulates XA21-mediated immunity and plant development in rice. Plant Mol. Biol. Report. **34:** 628–637.

Williams, S.J., et al. (2014). Structural basis for assembly and function of a heterodimeric plant immune receptor. Science **344:** 299–303.

Williams, S.J., Sornaraj, P., deCourcy-Ireland, E., Menz, R.I., Kobe, B., Ellis, J.G., Dodds, P.N., and Anderson, P.A. (2011). An autoactive mutant of the M flax rust resistance protein has a preference for binding ATP, whereas wild-type M protein binds ADP. Mol. Plant Microbe Interact. **24:** 897–906.

Xie, B., Wang, X., Zhu, M., Zhang, Z., and Hong, Z. (2011). *CalS7* encodes a callose synthase responsible for callose deposition in the phloem. Plant J. **65:** 1–14.

Xie, Z., Zhang, Z.L., Zou, X., Huang, J., Ruas, P., Thompson, D., and Shen, Q.J. (2005). Annotations and functional analyses of the rice WRKY gene superfamily reveal positive and negative regulators of abscisic acid signaling in aleurone cells. Plant Physiol. **137:** 176–189.

Xu, F., Kapos, P., Cheng, Y.T., Li, M., Zhang, Y., and Li, X. (2014). NLR-associating transcription factor bHLH84 and its paralogs function redundantly in plant immunity. PLoS Pathog. **10:** e1004312.

Yamaguchi, K., Yamada, K., and Kawasaki, T. (2013). Receptor-like cytoplasmic kinases are pivotal components in pattern recognition receptor-mediated signaling in plant immunity. Plant Signal. Behav. **8:** 4161–, 25662.

Yu, D., Chen, C., and Chen, Z. (2001). Evidence for an important role of WRKY DNA binding proteins in the regulation of *NPR1* gene expression. Plant Cell **13:** 1527–1540.

Zarate, S.I., Kempema, L.A., and Walling, L.L. (2007). Silverleaf whitefly induces salicylic acid defenses and suppresses effectual jasmonic acid defenses. Plant Physiol. **143:** 866–875.

Zhang, J., et al. (2010). Receptor-like cytoplasmic kinases integrate signaling from multiple plant immune receptors and are targeted by a Pseudomonas syringae effector. Cell Host Microbe **7:** 290–301.

Zhang, L., et al. (2015). Cryo-EM structure of the activated NAIP2-NLRC4 inflammasome reveals nucleated polymerization. Science **350:** 404–409.

Zhang, Y., Dorey, S., Swiderski, M., and Jones, J.D. (2004). Expression of *RPS4* in tobacco induces an AvrRps4-independent HR that requires EDS1, SGT1 and HSP90. Plant J. **40:** 213–224.

Zhao, Y., et al. (2016). Allelic diversity in an NLR gene *BPH9* enables rice to combat planthopper variation. Proc. Natl. Acad. Sci. USA **113:** 12850–12855.

Zhou, X., Wang, J., Peng, C., Zhu, X., Yin, J., Li, W., He, M., Wang, J., Chern, M., Yuan, C., Wu, W., and Ma, W., et al. (2016). Four receptor-like cytoplasmic kinases regulate development and immunity in rice. Plant Cell Environ. **39:** 1381–1392.

Zhou, Y.L., Xu, M.R., Zhao, M.F., Xie, X.W., Zhu, L.H., Fu, B.Y., and Li, Z.K. (2010). Genome-wide gene responses in a transgenic rice line carrying the maize resistance gene *Rxo1* to the rice bacterial streak pathogen, *Xanthomonas oryzae* pv. *oryzicola.* BMC Genomics **11:** 78.

Zhu, Z., Xu, F., Zhang, Y., Cheng, Y.T., Wiermer, M., Li, X., and Zhang, Y. (2010). *Arabidopsis* resistance protein SNC1 activates immune responses through association with a transcriptional corepressor. Proc. Natl. Acad. Sci. USA **107:** 13960–13965.

Zipfel, C. (2014). Plant pattern-recognition receptors. Trends Immunol. **35:** 345–351.